

Th_2O^- , Th_2Au^- , and $\text{Th}_2\text{AuO}_{1,2}^-$ Anions: Photoelectron Spectroscopic and Computational Characterization of Energetics and Bonding

Zhaoguo Zhu, Mary Marshall, Rachel M. Harris, Kit H. Bowen,* Monica Vasiliu, and David A. Dixon*



Cite This: *J. Phys. Chem. A* 2021, 125, 258–271



Read Online

ACCESS |

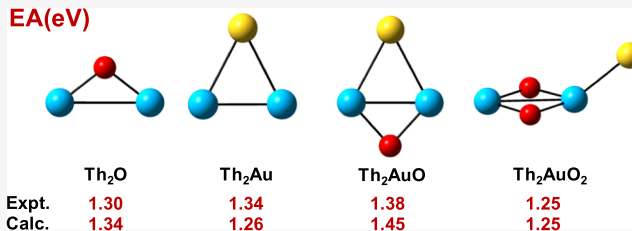
Metrics & More

Article Recommendations

Supporting Information

ABSTRACT: The observation and characterization of the anions: Th_2O^- , Th_2Au^- , and $\text{Th}_2\text{AuO}_{1,2}^-$ is reported. These species were studied through a synergistic combination of anion photoelectron spectroscopy and ab initio correlated molecular orbital theory calculations at the CCSD(T) level with large correlation-consistent basis sets. To better understand the energetics and bonding in these anions and their corresponding neutrals, a range of smaller diatomic to tetratomic species were studied computationally. Correlated molecular orbital theory calculations at the CCSD(T)

level showed that in most of these cases, there are close-lying anions and neutral clusters with different geometries and spin states and are consistent with the experimentally observed spectra. Thus, comparison of experimentally determined and computationally predicted vertical detachment energies and electron affinities for different optimized geometries and spin states shows excellent agreement to within 0.1 eV. The structures for both the neutrals and anions have a significant ionic component to the bonding because of the large electron affinity of the Au atom and modest ionization potentials for Th_2 , Th_2O , and Th_2O_2 . The analysis of the bonding for the Th–Th bonds from the molecular orbitals is consistent with this ionic model. The results show that there is a wide variation in the bond distance from 2.7 to 3.5 Å for the Th–Th bonds all of which are less than twice the atomic radius of Th of 3.6 Å. The bond distances encompass bond orders from 4 to 0. There can be different bond orders for the same bond distance depending on the nature of the ionic bonding suggesting that one may not be able to correlate the bond order with the bond distance in these types of clusters. In addition, the presence of an Au atom may provide a unique probe of the bonding in such clusters because of its ability to accept an electron from clusters with modest ionization potentials.



INTRODUCTION

Most of the actinides have valence electrons residing in 5f-orbitals, giving them chemical properties that are unlike those of other families in the periodic table. The actinides can also have multiple oxidation states, ranging from +2 to +7, leading to diverse molecular geometries. Because of their electronic configurations, the actinides are capable of bonding that is not typically observed in transition metal chemistry. Bonding in the actinides can often follow different trends, for example, bond lengths decreasing with increasing atomic number.¹ This is the result of the well-known actinide contraction, by which their 5f orbitals become more stable (and more contracted) with increasing atomic number.^{2,3} Also, whereas metal–metal bonds are common among the d-block metals, very few such bonds have been observed in the actinide series.⁴ Even so, actinides can form multiple covalent molecular bonds.^{5–7} A better understanding of the electronic structure and bonding behavior of the actinides is necessary in order to advance the development of nuclear energy-related applications, generally and the management of its resulting waste products, in particular.

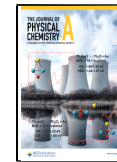
Thorium is the second element in the actinide series with the electronic configuration, $[\text{Rn}]6d^27s^2$, with four valence electrons. Because of the fact that it uses its 7s and 6d orbitals for bonding, thorium's chemistry often resembles that of the

transition metals. Metal–metal bonds between thorium atoms have been investigated extensively through quantum chemistry. Straka and Pyykkö performed a quasirelativistic density functional (B3LYP) calculation on the HThThH molecule, predicting that the ${}^1\Sigma_g$ ground state has a triple Th–Th bond with a bond length of 2.71 Å.⁸ In 2006, Th_2 was predicted to have a quadruple bond character with a ${}^3\Delta_g$ ground state.⁶ Twelve low-lying excited states within an energy range of less than 1 eV were predicted with the first excited ${}^1\Sigma_g^+$ state only 400 cm⁻¹ above the ground state. It was predicted that a quadruple bond is present in both its ground and first excited states. Also through computations, a variety of ligands have been used to probe the Th–Th bond length in LThThL molecules [$\text{L} = \text{C}_8\text{H}_8$,⁹ $\text{C}_5(\text{CH}_3)_5$,¹⁰ and NH_3 , PH_3 , PMe_3 , PCy_3 , PPh_3 , AsH_3 , NHC , CO , and NO .⁴] To date, the $\text{H}_3\text{AsThThAsH}_3$ molecule has been predicted to have the shortest Th–Th quadruple bond

Received: October 29, 2020

Revised: December 2, 2020

Published: December 16, 2020



length (2.590 Å).⁴ Ligand substitutions can tune the Th–Th bond order (BO) from quadruple ($H_3AsThThAsH_3$), to triple ($H_3NThThNH_3$), to double (OCThThCO), and to single (ONThThNO). Th–Th bonds confined in carbon cages have also been modeled. Ge et al. predicted a stable Th(III)-based dimetallofullerene, $Th_2@I_h-C_{80}$, which consists of a Th_2^{6+} core and an $I_h-C_{80}^{6-}$ cage.¹¹ The two remaining valence electrons in the Th_2^{6+} core form open-shell, 2-fold, one-electron-two-center bonds with the electronic configuration of $(6d7s7p)\sigma^1(5f6d)\pi^1$. These authors further predicted that the Th–Th distance can be changed from 3.803 to 2.843 Å by replacing the I_h-C_{80} cage with the I_h-C_{60} cage. Correlated molecular orbital (MO) theory calculations have been reported for ThO_2 , ThO_2^- , Th_2O_2 , and $Th_2O_4^{12}$.

In sharp contrast to the relatively extensive computational work on Th–Th bonding, experimental studies have been scarce. The only molecule to have been synthesized with a direct Th–Th bond appears to be the Th_2 molecule. This gas-phase Th_2 dimer was produced by laser ablation and detected by mass spectrometry.¹³ In 2015, it was studied in the gas phase via 2-D fluorescence spectroscopy; there, the vibrational frequencies for two of its electronically excited states (169 and 212 cm⁻¹) were compared to that of the ground state (135 cm⁻¹).¹⁴ These results suggest that Th_2 excited states have stronger Th–Th bonds than its ground state.

In addition to metal dimer and ligand-supported molecules, such as LMML (M = metal, L = ligand), heterometallic clusters with three or more metals in close proximity also contain metal–metal bonds.¹⁵ Several examples of M_nAu (M = metal, $n \geq 2$) clusters with short metal–metal bonds have been reported, these including those with M = Na,¹⁶ Ti,¹⁷ Cr,¹⁸ Cu,¹⁹ Ag,²⁰ Pt,²¹ and La, Y, and Sc.²² Nevertheless, despite the abundance of data on these heterometallic clusters, the literature is moot on M_nAu species in which M = Th. In the present study, however, we report the observation of the anions, Th_2O^- , Th_2Au^- , $Th_2AuO_1^-$, and $Th_2AuO_2^-$, in the gas phase. These anions were characterized by time-of-flight mass spectrometry, anion photoelectron spectroscopy, and ab initio electronic structure calculations. The synergistic combination of anion photoelectron spectroscopy and computations showed that Th–Th metal–metal bonds are formed in all four of these species. Additionally, this work revealed that the bonding character between thorium and gold is significantly influenced by oxygen, evolving from metallic toward ionic bonding when oxygen is present.

METHODS

Experimental Section. This work utilized anion photoelectron spectroscopy (aPES) as its primary experimental tool. The aPES technique is conducted by crossing a mass-selected beam of negative ions with a fixed-energy photon beam and energy analyzing the resulting photodetached electrons. This technique is governed by the energy-conservation relationship, $h\nu = EBE + EKE$, where $h\nu$, EBE, and EKE are the photon energy, electron binding (photodetachment transition) energy, and the electron kinetic energy, respectively. Our photoelectron spectrometer, which has been described previously,²³ consists of an ion source, a linear time-of-flight (TOF) mass spectrometer, a mass gate, a momentum decelerator, a neodymium-doped yttrium aluminum garnet (Nd:YAG) laser for photodetachment, and a magnetic bottle electron energy analyzer. Photoelectron spectra were calibrated against the well-known photoelectron spectrum of Cu^- .²⁴

The anions of interest were generated using a pulsed-arc (electric discharge) cluster ionization source (PACIS), which has been described in detail elsewhere.^{25,26} This cluster anion source has been used to generate a variety of bimetal cluster anions.^{27–31} During PACIS operation, a 30 μs long, 150 V electrical pulse applied between a copper anode and the sample cathode vaporizes the sample atoms. The sample cathode was prepared in a nitrogen glove box, where the sample powder was firmly pressed onto an aluminum rod. Both pure thorium powder and a 3:1 Th/Au powder mixture were used in the experiment. To prevent contact between the thorium powder and air, a thin sacrificial layer of aluminum powder was pressed onto the top of the sample layer. During operation of the PACIS source and almost simultaneously with the firing of its electric discharge pulses, ~150 psi of ultrahigh purity helium gas was injected into the source's discharge region through a pulsed valve, these actions together result in the generation of a variety of cluster sizes and compositions. The Th_2O^- anions were generated using a pure thorium powder sample, while the thorium-gold-containing clusters anions were formed using a thorium-gold mixed powder sample. The resulting plasma, containing ions, neutrals, and electrons, was cooled as it expanded through the PACIS source's housing and nozzle. The resulting anion mixture was mass analyzed by TOF mass spectroscopy, after which the chosen mass-selected anion compositions were photodetached and their resulting electrons were energy analyzed.

Computational Methods. All cluster geometries were initially optimized at the DFT level³² with the hybrid B3LYP exchange correlation functional.^{33,34} The aug-cc-pVDZ basis sets^{35,36} were used for O, the cc-pVDZ-PP basis sets with effective core potentials were used for Th,^{37,38} and the aug-cc-pVDZ-PP basis sets with effective core potentials were used for Au.³⁹ Vibrational frequencies were calculated to confirm that the structures were minima. These calculations were performed using the Gaussian16 program system.⁴⁰

The DFT geometries were then used as starting points for high accuracy coupled cluster theory with single and double excitations with perturbative triples correction [CCSD(T)]^{41–44} calculations to predict the structural characteristics for the lower-energy isomers and the energetics. The aug-cc-pVnZ basis sets were used for O, the cc-pVnZ-PP basis sets were used for Th, and aug-cc-pVnZ-PP were used for Au for $n = D, T$, and Q. These basis sets are abbreviated as an for $n = D, T$, and Q. The CCSD(T) energies were extrapolated to the CBS limit by fitting to a mixed Gaussian/exponential (eq 1)^{45,46}

$$E(n) = E_{CBS} + A \exp[-(n - 1)] + B \exp[-(n - 1)^2] \quad (1)$$

where $n = 2, 3$, and 4 (DZ through QZ). Values obtained from this procedure are denoted as CBS.

The lower-energy isomers were optimized at the CCSD(T) at up to $n = T$, except for $Th_2AuO_2^{0/-}$ clusters, which were optimized at $n = D$ level. For the diatomics, a 7-point Dunham expansion was used.^{47,48} The diatomic harmonic frequencies (ω_e) and anharmonic constants ($\omega_e\chi_e$) were also calculated. The thermodynamic properties were predicted using the CCSD(T)/aT (or aD for the largest ones) optimized geometries at the CCSD(T) level of theory including core-valence (CV) correlation corrections with the aug-cc-pwCVnZ(O)/cc-pwCVnZ-PP(Th)/aug-cc-pwCVnZ-PP(Au) basis sets for $n = D, T$, and Q (abbreviated as awn for $n = D, T$ and Q). The calculations included the correlation of the valence electrons and

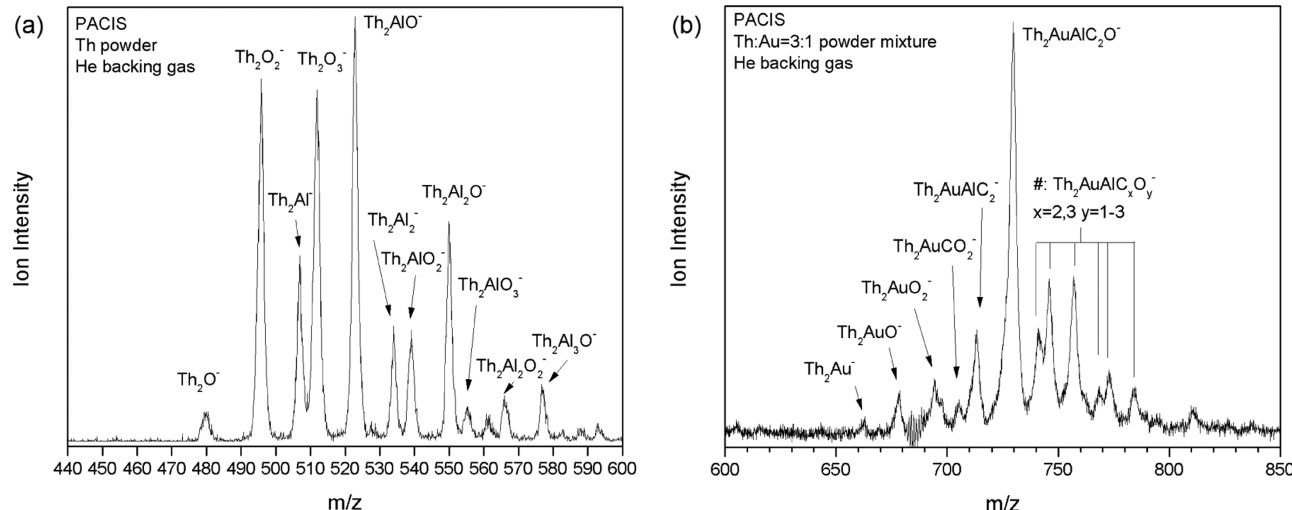


Figure 1. The mass spectra of anions generated by PACIS when using (a) thorium powder and helium gas and (b) a 3:1 thorium-gold powder mixture and helium gas.

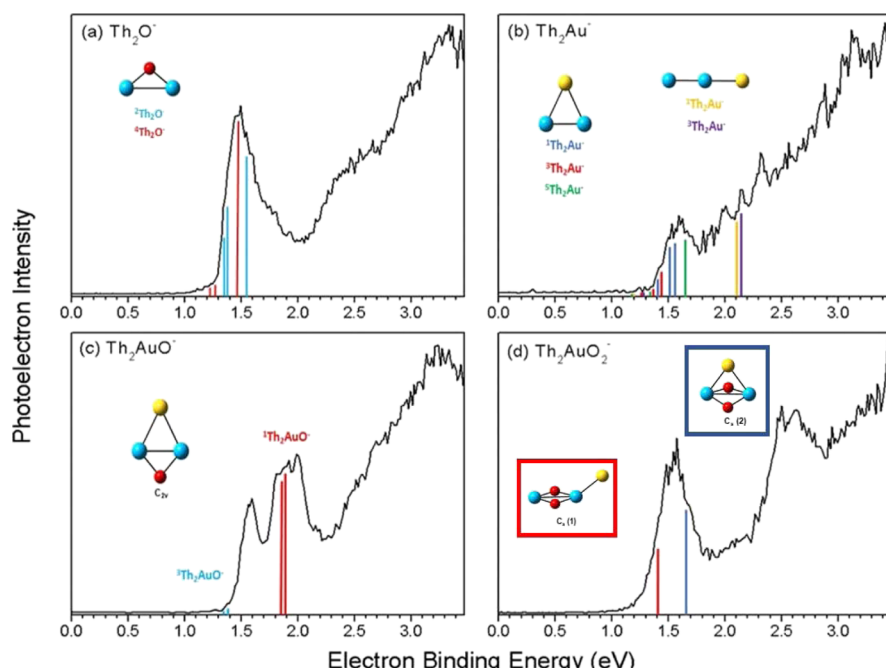


Figure 2. Photoelectron spectra of (a) Th_2O^- , (b) Th_2Au^- , (c) Th_2AuO^- , and (d) $\text{Th}_2\text{AuO}_2^-$ measured with 3.49 eV photons. Lowest energy isomeric structures are displayed for each species, with thorium in blue, gold in yellow, and oxygen in red. Calculated VDEs (eV) at the CCSD(T)/aT level for each structure are indicated by colored bars.

the outer core electrons (5d, 6s, and 6p core–shell electrons for Th, 5s, and 5p core–shell electrons for Au and the 1s core–shell electrons of O).

Total atomization energies (TAEs or ΣD_0) at 0 K were calculated from the following expression (eq 2) with Δ referring to the difference between the molecule (reactant) and the atomic products for each energy component using aug-cc-pwCVnZ(O)/cc-pwCVnZ-PP(Th)/aug-cc-pwCVnZ-PP(Au) basis sets for $n = \text{D}, \text{T}$, and Q and the CBS extrapolation

$$\sum D_0 = \Delta E_{\text{CBS}} + \Delta E_{\text{ZPE}} + \Delta E_{\text{SO}} \quad (2)$$

Additional corrections to the CCSD(T)/CBS energy (ΔE_{CBS}) are necessary to reach chemical accuracy (± 1 kcal/mol). The unscaled vibrational frequencies from the B3LYP/aD

calculations were used to calculate the vibrational zero point energies (ZPEs) for all the molecules except the diatomic where the harmonic frequencies (ω_e) and anharmonic constants ($\omega_e x_e$) at the CCSD(T)/awQ level were used to calculate the ZPEs. The atomic spin–orbit corrections were used to calculate the spin orbit corrections of the molecules (ΔE_{SO}) with the O atom from Moore's tables⁴⁹ ($\Delta E_{\text{SO}}(\text{O}) = 0.22$ kcal/mol), and the Th atom from Sansonetti and Martin⁵⁰ ($\Delta E_{\text{SO}}(\text{Th}) = 8.81$ kcal/mol).

Heats of formation at 0 K were calculated by combining our computed ΣD_0 values with the known enthalpies of formation at 0 K for the elements with $\Delta H_{f,0K}(\text{O}) = 59.00 \pm 0.00$ kcal/mol, from the active thermochemical tables (ATcT),^{51–53} $\Delta H_{f,0K}(\text{Au}) = 88.0 \pm 0.5$ kcal/mol,⁵⁴ and $\Delta H_{f,0K}(\text{Th}) = 143.9 \pm 1.4$ kcal/mol.⁵⁵ Note that there is another value reported for

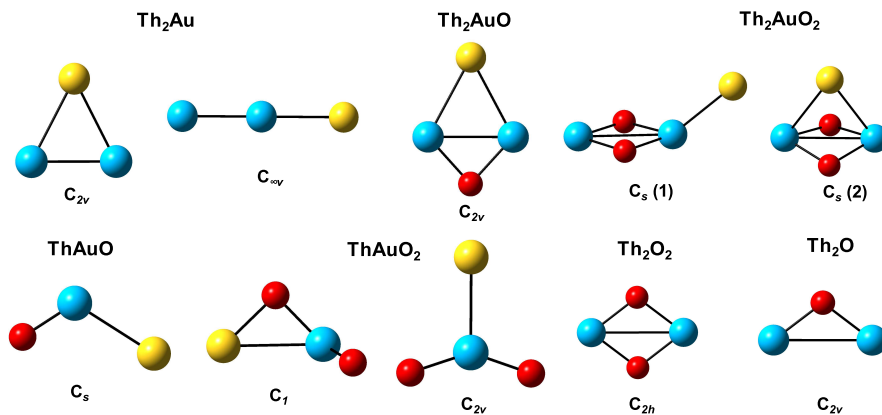


Figure 3. Lowest energy isomeric structures. Thorium in blue, Gold in yellow, and Oxygen in red.

$\Delta H_{f,0K}(\text{Th}) = 142.1 \pm 1.5 \text{ kcal/mol}$.⁵⁶ Heats of formation at 298 K were calculated by following the procedures outlined by Curtiss et al.⁵⁷ using 1.3 kcal/mol thermal corrections for Au and Th, respectively, and 1.04 kcal/mol thermal corrections for O.

The open-shell calculations were done with the R/UCCSD(T) approach where a restricted open shell Hartree-Fock (ROHF) calculation was initially performed and the spin constraint was then relaxed in the coupled cluster calculation.^{43,58–60} The CCSD(T) calculations were performed with the MOLPRO 2018 program package.^{61,62} The Natural Population Analysis (NPA) results based on the Natural Bond Orbitals (NBOs)^{63,64} using NBO7^{65,66} are calculated using MOLPRO 2018.

The calculations were done on our local UA Opteron- and Xeon-based Linux computation clusters as well as on using resources in the Molecular Sciences Computing Facility (MSCF) in the Environmental Molecular Science Laboratory (EMSL) at Pacific Northwest National Laboratory (PNNL) and the DMC computer at the Alabama Supercomputer Center.

RESULTS AND DISCUSSION

Experimental Results. Figure 1a presents the mass spectrum of cluster anions generated using thorium metal powder and helium expansion gas in a PACIS source. There, we observe the anionic clusters: $\text{Th}_2\text{O}_{1-3}^-$, $\text{Th}_2\text{AlO}_{0-3}^-$, $\text{Th}_2\text{Al}_2\text{O}_{0-2}^-$, and $\text{Th}_2\text{Al}_3\text{O}^-$. Figure 1b shows the mass spectrum of Th_2Au -containing cluster anions made from a thorium-gold powder mixture and helium expansion gas in a PACIS source. There, one observes the $\text{Th}_2\text{AuO}_{0-2}^-$ series, the $\text{Th}_2\text{AuCO}_2^-$ anion, and the $\text{Th}_2\text{AuAlC}_{2,3}\text{O}_{0-3}^-$ cluster anion series. This mass spectrum is simplified by the fact that thorium and gold each have only one naturally occurring isotope. The contaminant elements: aluminum, carbon, and oxygen, seen in these spectra originated from the surface of the cathode and the surroundings in the PACIS source housing. Because there were no mass-coincident species present at masses: 480, 661, 677, and 693 amu, these anions were identified as: Th_2O^- , Th_2Au^- , Th_2AuO^- , and $\text{Th}_2\text{AuO}_2^-$. Each of these was mass selected and their photoelectron spectra measured using third harmonic photons (355 nm, 3.49 eV/photon) from a Nd:YAG laser.

The photoelectron spectra of Th_2O^- , Th_2Au^- , Th_2AuO^- , and $\text{Th}_2\text{AuO}_2^-$ are presented in Figure 2. The photoelectron spectrum of Th_2O^- [see Figure 2a] exhibits a peak with an onset at EBE = 1.30 eV and an intensity maximum at EBE = 1.49 eV. An unresolved band has a shoulder ranging from EBE = 2.0 to 2.7 eV and a peak centered at EBE = 3.30 eV. The

photoelectron spectrum of Th_2Au^- , [see Figure 2b], exhibits a peak with an onset at EBE = 1.34 eV and an intensity maximum at EBE = 1.60 eV. The series of poorly resolved peaks beyond EBE = 1.7 eV correspond to transitions from the ground state of the anion to the various electronically excited states of the Th_2Au^- anion's neutral counterpart. The photoelectron spectrum of Th_2AuO^- , [see Figure 2c], displays a peak that is centered at EBE = 1.59 eV. The fact that this peak is narrower than the lowest EBE peak in the photoelectron spectrum of Th_2Au^- suggests that the geometric structures of Th_2AuO^- and Th_2AuO are more similar to each other than are the geometric structures of Th_2Au^- and Th_2Au . The second band in the Th_2AuO^- spectrum ranges from EBE = 1.85 eV to EBE = 2.05 eV and reaches its maximum intensity at EBE \sim 2.0 eV. Beyond EBE = 2.3 eV, a broad band appears that rises steadily attaining its maximum intensity at EBE \sim 3.3 eV. The photoelectron spectrum of $\text{Th}_2\text{AuO}_2^-$ [see Figure 2d] exhibits two broad peaks with intensity maxima at EBE = 1.56 eV and EBE = 2.50 eV.

The vertical detachment energy (VDE) is the photodetachment transition at which the Franck-Condon overlap between the wave function of the ground state of the anion and that of the ground state of its neutral counterpart is maximal. Thus, the VDE value corresponds to the EBE value of the intensity maximum of the lowest EBE peak. The VDE values of Th_2O^- , Th_2Au^- , Th_2AuO^- , and $\text{Th}_2\text{AuO}_2^-$ are, therefore, 1.49, 1.60, 1.59, and 1.56 eV, respectively. The adiabatic (thermodynamic) electron affinity (EA) is the energy difference between the lowest energy state of the anion and the lowest energy state of its neutral counterpart. When sufficient Franck-Condon overlap exists between $v = 0$ of the anion and $v' = 0$ of its neutral counterpart (the origin transition) and there are no vibrational hot bands (photoelectrons from vibrationally excited anions) present, the EA value corresponds to the EBE value at the intensity threshold of the lowest EBE peak or band. We have assigned EA values by extrapolating the low EBE side of the lowest EBE bands to zero. The EA values for Th_2O , Th_2Au , Th_2AuO , and Th_2AuO_2 are, therefore, 1.30, 1.34, 1.38, and 1.25 eV, respectively. The EA values of these four species, as well as their VDE values, are relatively similar to one another.

Computational Results. A variety of structures and spin states were examined for the anions: Th_2Au^- , Th_2AuO^- , and $\text{Th}_2\text{AuO}_2^-$ and their corresponding neutrals. In addition, we also predicted the properties of Th_2 , ThAu , ThAuO , ThAuO_2 , AuO , AuO_2 , Th_2O , Th_2O_2 , and ThO_2 and their anions for comparison as well as the EAs of atomic Th and Au. Selected low-energy structures are shown in Figure 3.

Table 1. Relative Energies of Th₂Au and Th₂Au⁻ in kcal/mol at Different Levels of Theory^a

isomer	B3LYP/aD	CCSD(T)/aD (sp)	CCSD(T)/aD (opt)	CCSD(T)/aT (sp)	CCSD(T)/aT (opt)	CCSD(T)/aQ (sp)	CCSD(T)/CBS	CCSD(T)/awD/T/Q/CBS ^b
² Th ₂ Au (C _{2v})	13.4	0.2	0.0	0.0	0.0	0.0	0.0	0.0/0.3/0.6/0.7
⁴ Th ₂ Au (C _{2v})	11.2	1.1	1.3	2.9				
⁶ Th ₂ Au (C _{2v})	10.4	3.6		6.1				
² Th ₂ Au (C _{∞o})	0.0	0.0	0.1	0.2	0.4	0.7	0.8	0.0
⁴ Th ₂ Au (C _{∞o})	11.8	20.8						
² Th ₂ Au (D _{∞oh})	67.2							
¹ Th ₂ Au ⁻ (C _{2v})	1.6	0.0	0.0	0.0	0.0	0.0	0.0	0.0
³ Th ₂ Au ⁻ (C _{2v})	5.8	2.9		3.5				
⁵ Th ₂ Au ⁻ (C _{2v})	4.7	3.0		2.1				
¹ Th ₂ Au ⁻ (C _{∞o})	0.0	1.7	2.6	1.1	1.1	0.4	0.0	3.1/2/1/1.2/0.6
³ Th ₂ Au ⁻ (C _{∞o})	0.3	3.7		2.3				
¹ Th ₂ Au ⁻ (D _{∞oh})	52.9							

^asp = single-point calculations (no geometry optimization); opt = geometry optimization. ^bCCSD(T)/aT optimized geometries were used.

Table 2. Relative Energies of Th₂AuO, Th₂AuO⁻, Th₂AuO₂, and Th₂AuO₂⁻ in kcal/mol at Different Levels of Theory^a

isomer	B3LYP/aD	CCSD(T)/aD (sp)	CCSD(T)/aD (opt)	CCSD(T)/aT ^b	CCSD(T)/aQ	CCSD(T)/CBS	CCSD(T)/awD/T/Q/CBS ^c
Th ₂ AuO/Th ₂ AuO ⁻							
² Th ₂ AuO (C _{2v})	4.1	0.7	0.3	0.0	0.0	0.0	0.5/0.0/0.0/0.0
⁴ Th ₂ AuO (C _{2v})	0.0	0.0	0.0	1.7	3.0	3.8	0.0/0.6/1.7/2.3
¹ Th ₂ AuO ⁻ (C _{2v})	0.0	0.0	0.0	0.0	0.0	0.0	0.0
³ Th ₂ AuO ⁻ (C _{2v})	3.1	3.8	4.8	3.6	2.4	1.7	5.6/5.6/4.3/3.4
Th ₂ AuO ₂ /Th ₂ AuO ₂ ⁻							
² Th ₂ AuO ₂ (C _s) (1)	0.0	0.0		0.0			
⁴ Th ₂ AuO ₂ (C _s) (1)	18.1	22.1		22.4			
² Th ₂ AuO ₂ (C _s) (2)	21.0	21.0		21.0			
⁴ Th ₂ AuO ₂ (C _s) (2)	23.1	28.6		27.6			
¹ Th ₂ AuO ₂ ⁻ (C _s) (1)	0.0	0.0	0.0	0.0	0.0	0.0	0.0
¹ Th ₂ AuO ₂ ⁻ (C _s) (2)	6.8	3.8	3.9	4.0	4.1	4.2	2.4/2.9/3.7/4.2
³ Th ₂ AuO ₂ ⁻ (C _s) (1)	8.0	13.2		12.6			
³ Th ₂ AuO ₂ ⁻ (C _s) (2)	23.2	22.4		21.8			

^asp = single-point calculations (no geometry optimization); opt = geometry optimization. ^bCCSD(T)/aT (opt) for Th₂AuO and CCSD(T)/aT (sp) for Th₂AuO₂. ^cCCSD(T)/aT optimized geometries were used for Th₂AuO and CCSD(T)/aD optimized geometries were used for Th₂AuO₂.

Table 3. Th₂O and Th₂O⁻ Relative Energies in kcal/mol at Different Levels of Theory^a

isomer	B3LYP/aD	CCSD(T)/aD (opt)	CCSD(T)/aT (opt)	CCSD(T)/aQ	CCSD(T)/CBS	CCSD(T)/awD/T/Q/CBS ^b
³ Th ₂ O (C _{2v})	0.0	0.0	0.0	0.0	0.0	0.0
⁵ Th ₂ O (C _{2v})	2.5	2.2	1.2	0.5	0.0	1.7/2.2/1.4/0.8
¹ Th ₂ O (C _{2v})	7.4	4.4	4.1	4.0	3.8	4.4/4.1/4.1/4.0
³ Th ₂ O (C _s) (ThThO)	25.3					
² Th ₂ O ⁻ (C _{2v})	0.0	0.0	0.0	0.0	0.0	0.0
⁴ Th ₂ O ⁻ (C _{2v})	0.4	2.0	3.0	3.5	3.9	2.2/3.0/3.4/3.7
⁶ Th ₂ O ⁻ (C _{2v})	16.5	20.6 (sp)	21.6 (sp)			

^asp = single-point calculations (no geometry optimization); opt = geometry optimization. ^bCCSD(T)/aT optimized geometries were used.

Geometries and Isomer Energies. Relative energies of various isomers and in different spin states are given in Tables 1–4. The optimized geometric parameters for the Th–Th bonds are given in Table 5 with the remaining data in the Supporting Information.

Th₂AuO_{0–2}. Th₂Au and its anion have a complicated set of states and geometries. The lowest energy state for Th₂Au⁻ is either ¹A₁ in C_{2v} symmetry or the linear singlet ThThAu; these two isomeric structures being different by less than 1 kcal/mol.

At the highest computational level, that is, CCSD(T)/CBS with weighted core basis sets, the linear singlet is 0.6 kcal/mol above the C_{2v} singlet. The triplet and quintet states for the C_{2v} isomer are, at most, 3.5 kcal/mol higher in energy. The triplet state for the linear ThThAu isomer is also close in energy. Thus, there will be a significant number of species observed in the experiment, which have comparably low energies.

For neutral Th₂Au, there are again two very low-energy doublet structures within 1 kcal/mol of each other. Linear

Table 4. Th₂ and Th₂⁻ Relative Energies in kcal/mol at Different Levels of Theory^a

isomer	B3LYP/aD	CCSD(T)/aD	CCSD(T)/aT	CCSD(T)/aQ	CCSD(T)/CBS	CCSD(T)/awD	CCSD(T)/awT	CCSD(T)/awQ	CCSD(T)/CBS
³ Th ₂	0.0	0.5	0.0	0.0	0.0	0.4	0.0	0.0	0.0
¹ Th ₂	3.8	0.0	0.3	0.5	0.7	0.0	0.3	0.5	0.6
⁵ Th ₂	11.8	5.9	9.2						
² Th ₂ ⁻	6.2	2.3	0.0	0.0	0.0	2.2	0.6	0.0	0.0
⁴ Th ₂ ⁻	0.0	6.8	3.8	3.6	3.5	6.6	4.6	3.6	3.0
⁶ Th ₂ ⁻	8.9	0.0	0.2	1.5	2.3	0.0	0.0	0.1	0.5

^aAll CCSD(T)/aT optimized geometry.

Table 5. Th–Th BO Analysis from NBO and MO Analysis

molecule	r(Th–Th) (Å)	NBO BO	MO BO
² Th ₂ Au (C_{2v})	2.765	3.48	3.5
² Th ₂ Au ($C_{\infty v}$)	2.720	2.93	3.5
¹ Th ₂ Au ⁻ (C_{2v})	2.990	1.92	3.0
¹ Th ₂ Au ⁻ ($C_{\infty v}$)	2.773	2.92	4.0
² Th ₂ AuO (C_{2v})	2.888	2.48	2.5
⁴ Th ₂ AuO (C_{2v})	3.057	1.48	2.0
¹ Th ₂ AuO ⁻ (C_{2v})	3.443	0.97	1.0
³ Th ₂ AuO ⁻ (C_{2v})	2.972	1.98	2.5
² Th ₂ AuO ₂ (C_s) (1)	3.383	0.00	0.0
¹ Th ₂ AuO ₂ ⁻ (C_s) (1)	3.419	0.00	0.0
¹ Th ₂ AuO ₂ ⁻ (C_s) (2)	3.342	0.00	0.0
³ Th ₂ O (C_{2v})	3.324	0.50	2.0
⁵ Th ₂ O (C_{2v})	3.056	1.97	2.0
¹ Th ₂ O (C_{2v})	3.364	1.00	2.0
² Th ₂ O ⁻ (C_{2v})	3.170	1.48	2.5
⁴ Th ₂ O ⁻ (C_{2v})	3.144	1.47	1.5
¹ Th ₂ O ₂ (C_{2h})	3.350	0.00	0.0
² Th ₂ O ₂ ⁻ (C_{2v})	3.382	0.00	0.0
³ Th ₂	2.694	4.00	4.0
¹ Th ₂	2.736	4.00	4.0
² Th ₂ ⁻	2.683	4.50	3.5
⁴ Th ₂ ⁻	2.680	4.50	4.0
⁶ Th ₂ ⁻	2.782	3.50	4.0

ThThAu is 0.7 kcal/mol less stable than the C_{2v} structure at the CCSD(T)/CBS limit with weighted core basis sets. There are also low-energy quartet and sextet states for the C_{2v} isomer of the neutral. Thus, the VDEs and the adiabatic EA will be complicated by the number of low-lying species in both the neutral and its anion, as will the geometries of the various species.

The Th–Th bond distances for Th₂Au⁻ and Th₂Au are given in Table 5 (See Figure 3 for structures). For the C_{2v} geometries of both the anion and its neutral, the Th–Th bond length is very sensitive to the apical angle at Au; a slight increase in the \angle ThAuTh angle can lead to a significant increase in the Th–Th bond distance. For the C_{2v} geometry of the neutral, the Th–Th bond distance increases as the spin state increases, but no such trend is observed for the anion. For the linear ThThAu geometry, the Th–Th bond distance decreases as the spin state increases in its anion, whereas in its neutral, the Th–Th bond distance increases as the spin state increases, although to a lesser extent. The Th–Au bond distances are not strongly dependent on spin states for both the anion and its neutral in all the isomeric structures. The Th–Au bond distances are slightly longer in the anionic structures compared to their corresponding neutrals.

The addition of a single oxygen atom to Th₂Au leads to a wide range of structures. The O atom can bridge the Th–Th bond,

leading to different structures or it can add directly to a Th or Au atom external to the ring of metal atoms. The lowest energy structures all involve the O atom interacting with Th because the interaction of O with Au would involve a very high-energy species. This is consistent with the high bond energy for ThO at 208.5 kcal/mol¹¹ and the much lower BDE (bond dissociation energy) for AuO at 53.5 ± 5 kcal/mol.⁵³ The lowest energy structure for the anion is the singlet C_{2v} structure with the O atom bridging the Th–Th bond and with the Au atom bridging Th–Th bond opposite to the O atom. The triplet is less than 6 kcal/mol higher in energy, depending on the level of the theory. The lowest energy structure for the neutral is also a C_{2v} structure with the O atom bridging the Th–Th bond and the Au atom bridging the same Th–Th bond opposite to the O atom. The exact spin state depends on the level of the calculation with the quartet slightly higher in energy than the doublet (<4 kcal/mol) at the highest computational levels. The next higher energy isomeric neutral doublet structure has the O atom bridging the Th–Th bond and the Au atom binding only one Th atom. This structure could not be optimized for the anion.

The addition of an O atom bridging the Th–Th bond does not substantially change the geometry of the Th₂Au core for the neutral. Thus, Th–Au is essentially unchanged, and the Th–Th bond is ~ 0.17 Å longer in Th₂AuO as compared to Th₂Au. For the anion, Th₂AuO⁻, the Th–Au bond is ~ 0.11 Å shorter and the Th–Th bond is 0.45 Å longer than for the corresponding lowest energy Th₂Au⁻ structure. As observed for Th₂Au, the Th–Th bond is the most sensitive to the Th–Au–Th angle as well as the Th–O–Au angle. Thus, for the Th₂AuO⁻, C_{2v} structure, as the Th–Au–Th and Th–O–Au angles decrease from the lowest energy singlet to the triplet state, the Th–Th bond shortens by 0.47 Å, the Th–Au bond increases by 0.15 Å, and the Th–O bond stays almost the same. For neutral Th₂AuO, both Th–Au–Th and Th–O–Au angles increase from the doublet to the quartet state and the Th–Th bond increases by ~ 0.10 Å, although both the Th–Au and Th–O bonds change by less than 0.01 Å.

Addition of a second oxygen atom to Th₂AuO leads to the formation of a Th₂O₂ core with the Au now bonded to just one of the Th atoms and no longer bridging them as in the lowest energy structure. This structure for the anion is lower in energy by 4 kcal/mol than the one with the Au atom bridging the two Th atoms. For the neutral, the C_s (1) structure with two ThOTh bridges and the Au atom bonded to only one Th atom is clearly the most stable structure. The structure with the Au atom bridging both Th atoms, that is, C_s (2), is more than 20 kcal/mol higher in energy. For both anionic and neutral Th₂AuO₂ structures, the Th–Th bonds are much longer than predicted for Th₂Au and Th₂AuO and are comparable to the Th–Th bond in Th₂AuO⁻. The Th–Th–Au angle for the lowest energy Th₂AuO₂ anion is almost linear, but in the corresponding neutral, it bends to 138°. For the lowest energy anionic and

Table 6. CCSD(T) Adiabatic EAs (eV) (ΔH_{0K})

neutral	anion	aD/awD ^a	aT/awT ^a	aQ/awQ ^a	CBS/CBS ^a	expt.
² Th ₂ Au	¹ Th ₂ Au ⁻	1.35/1.36	1.26/1.32	1.23/1.28	1.22/1.26	1.34
² Th ₂ AuO	¹ Th ₂ AuO ⁻	1.51/1.55	1.45/1.55	1.39/1.49	1.36/1.45	1.38
² Th ₂ AuO ₂	¹ Th ₂ AuO ₂ ⁻	1.24/1.24	1.23/1.23	1.24	1.25	1.25
² ThAu	³ ThAu ⁻	0.96/0.92	1.02/0.96	1.05/0.99	1.07/1.01	
¹ Th ₂ O ₂	² Th ₂ O ₂ ⁻	0.50/0.47	0.50/0.45	0.52/0.47	0.54/0.49	
³ Th ₂ O	² Th ₂ O ⁻	1.21/1.22	1.28/1.25	1.34/1.30	1.38/1.34	1.30
¹ ThO ₂	² ThO ₂ ⁻	1.20/1.22	1.17/1.19	1.17/1.19	1.18/1.19	
² AuO ₂	³ AuO ₂ ⁻	3.35/3.32	3.42/3.40	3.47/3.46	3.50/3.49	
¹ ThO	² ThO ⁻	0.44/0.43	0.53/0.47	0.57/0.51	0.60/0.53	
² AuO	¹ AuO ⁻	2.15/2.20	2.28/2.33	2.34/2.38	2.37/2.41	2.3740 ± 0.0070 ⁶⁷
³ Th ₂	² Th ₂ ⁻	0.72/0.70	0.77/0.74	0.80/0.76	0.82/0.77	
³ Th	⁴ Th ⁻	0.45/0.44	0.53/0.51	0.60/0.56	0.64/0.59	0.607690(60) ⁶⁹
² Au	¹ Au ⁻	2.09/2.19	2.17/2.26	2.21/2.29	2.23/2.30	2.30860 ± 0.00070 ⁶⁸

^aBasis sets: cc-pVnZ-PP (Th), aug-cc-pVnZ-PP (Au), aug-cc-pVnZ (O)/aug-cc-pwCVnZ (O), cc-pwCVnZ-PP (Th), and aug-cc-pwCVnZ-PP (Au).

neutral Th₂AuO₂ structures, there are two different Th–O bonds, a longer one to the Th atom, which binds the Au atom and a shorter one, which links to the other Th atom.

Thorium Oxygen Species. For Th₂O, we cannot determine if the ground state is the triplet or the quintet because they have essentially the same energy; they are less than 1 kcal/mol apart at the CCSD(T)/CBS with weighted core basis set level of theory. Furthermore, the singlet is only 4 kcal/mol higher in energy. For the anion, the doublet is the ground state with the quartet being 4 kcal/mol higher in energy. The Th₂O anion and neutral have C_{2v} symmetry with the O atom bridging the Th–Th bond. For Th₂O⁻, the Th–Th bond distance is 3.17 Å and Th–O–Th angle is 97°; for Th₂O, the Th–Th bond distance is 0.15 Å longer and the angle is 105°. The Th–Th bonds become shorter as the Th–O–Th angle becomes smaller in going to the higher spin states, this being the case for both anions and neutrals. The Th–O bonds do not change as much as the Th–Th bond with the spin state, and they are slightly shorter for the neutrals compared to their corresponding anions.

While they were not studied experimentally in this work, it is nevertheless instructive to consider the related anions, Th₂O₂⁻ and ThAuO₀₋₂⁻, together with their neutral counterparts computationally. The lowest energy Th₂O₂⁻ anion and corresponding neutral have two O atom bridges on the Th–Th bond. The lowest energy Th₂O₂⁻ anion is a doublet state in C_{2v} symmetry with two shorter (2.07 Å) and two longer (2.21 Å) Th–O bonds. The quartet spin state is 14 kcal/mol higher in energy at the CCS(T)/aT level of theory. The lowest energy neutral, Th₂O₂, has a C_{2h} symmetry with four equivalent Th–O bonds of 2.11 Å length each. The triplet state neutral is 20 kcal/mol higher in energy at the CCS(T)/aT level of theory. The Th–Th bond distance is 3.38 Å for the lowest energy anion and 0.03 Å shorter for the neutral.

The ThO₂⁻ anion is a doublet in C_{2v} symmetry with a Th–O bond length of 1.95 Å and an O–Th–O angle of 114° at the CCSD(T)/aT level. The Th–O bond distances for the singlet neutral ThO₂ are ~0.04 Å shorter. ThO is predicted to be a singlet and ThO⁻ is predicted to be a doublet. The bond distance is predicted to increase from 1.85 Å in the neutral to 1.89 Å in the anion.

ThAuO₀₋₂. The dimer anion ThAu⁻ is predicted to have a triplet ground state, whereas neutral ThAu is predicted to be a doublet ground state. The ThAu⁻ singlet and quintet

states are 10 and 13 kcal/mol, respectively, higher in energy. The neutral ThAu quartet is about 6 kcal/mol higher in energy. The bond distance is predicted to increase from 2.71 Å in the neutral to 2.82 Å in the anion at the CCSD(T)/aQ level of theory. The Th–Au bond for both the neutral and the anion is not significantly dependent on the spin state, exhibiting changes less than 0.02 Å. The Th–Au bond distances in the anion and neutral ThAu dimer are ~0.20 and ~0.30 Å, respectively, these being shorter than in the corresponding Th₂Au structures.

The lowest energy structures of both the ThAuO⁻ anion and its neutral are bent. They have C_s symmetry, with Th serving as the central atom and with Au binding to the ThO moiety. The ThAuO⁻ anion is a ground state singlet, with its triplet state residing at least 26 kcal/mol higher in energy. Neutral ThAuO is a doublet ground state, with its other spin states sitting much higher in energy. The Th–Au bond distance for the anion is 2.93 Å, that is, ~0.13 Å longer than for the neutral. The Th–O bond distance is almost unchanged, that is, 1.89 Å for the anion versus 1.86 Å for the neutral. The Th–Au bond distances for ThAuO⁻ and ThAuO are 0.05 Å longer and 0.21 Å shorter than for the corresponding Th₂AuO⁻ and Th₂AuO species. The Th–O bond distances for both ThAuO⁻ and ThAuO are much shorter than those of anionic and neutral Th₂AuO structures, where an O atom bridged both Th atoms; they are in fact similar to Th–O bonds in ThO dimers.

ThAuO₂⁻ has a singlet ground state in C_{2v} symmetry and a structure where an Au atom binds a ThO₂⁻-like molecule with an O–Th–O angle of 121°. The neutral, lowest energy ThAuO₂ isomer is a doublet in C₁ symmetry, with one of the O atoms bridging the Th–Au bond and the other O atom bonding only to Th. The ThAuO₂ isomer corresponding to the anion's lowest energy structure is about 8 kcal/mol higher in energy with an O–Th–O angle of ~144°. The Th–Au bond distance is 3.08 Å in the anion and ~0.1 Å shorter in the neutral. The Th–O bond distance for the anion is similar to the Th–O bond distance in ThO₂⁻.

Th₂ Dimer. The Th₂ dimer is complicated. The triplet is predicted to be the ground state for the neutral, but the singlet is only 0.6 kcal/mol higher in energy at the CCSD(T)/CBS level with the weighted core basis sets. At our best computational level, the CCSD(T)/CBS level with the weighted core basis sets, the Th₂⁻ anion is predicted to be a doublet ground state with the sextet and the quartet only 0.5 and 3.0 kcal/mol, respectively,

higher in energy. At the CCSD(T)/aQ level of theory, triplet Th_2 is predicted to have a bond distance of 2.69 Å, which is 0.04 Å shorter than in the singlet. For the doublet Th_2^- anion, the bond distance is 2.68, 0.01 Å shorter than the bond distance in the lowest energy ground state triplet neutral. The sextet Th_2^- anion has a longer bond distance of 2.78 Å, almost 0.10 Å longer than in the doublet anion ground state. The quartet anion is predicted to have almost the same bond distance as the doublet ground state.

Au Oxygen Species. AuO is predicted to have a singlet ground state and AuO^- is predicted to be a doublet. The bond distance in AuO^- is predicted to decrease to 1.88 from 1.89 Å in the neutral. AuO_2 is predicted to be linear with the doublet clearly being the ground state at the CCSD(T) level of theory. Its anion is a linear triplet with the singlet ~11 kcal/mol higher in energy. The Au–O distance is predicted to decrease from 1.85 Å in the anion to 1.80 Å in the neutral.

Calculated EAs and VDEs. The adiabatic EAs are summarized in Table 6 at the CCSD(T) level of theory with the DFT/B3LYP values reported in the Supporting Information. The calculated adiabatic EA for Th_2Au is 0.08 eV lower than the experimental value at the weighted core CCSD(T)/CBS level and 0.12 eV lower without the weighted core basis sets at the CCSD(T)/CBS level. The EA for Th_2AuO is 0.07 eV higher than the experimental value at the weighted core CCSD(T)/CBS level and 0.02 eV lower without the weighted core basis sets at the CCSD(T)/CBS level. The calculated CCSD(T)/CBS EA for Th_2AuO_2 is the same as the experimentally determined value. The calculated adiabatic EA for Th_2O at the CCSD(T)/CBS level with and without weighted core basis sets is 0.04 and 0.08 eV, respectively, greater than the experimental values. The agreement between computational and experimental values confirms the spectral assignments of the adiabatic EAs.

As additional benchmarks of our approach, the experimental EAs of AuO^{67} and Au^{68} are also known, with the calculated values falling within 0.04, and 0.01 eV of the experimental values. The calculated value for Th is within 0.01 eV of the recently reported experimental value.⁶⁹ This good agreement with experiment further confirms that our calculated results should be valid to better than ± 0.1 eV. Note that for ${}^4\text{Th}^-$, there are two states very close in energy, $(6d\sigma)^1(6d\delta)^1(6d\pi)^1$ and $(6d\delta)^1(6d\pi)^2$, with the first one of these just 1.3 kcal/mol higher in energy.

The VDEs are given in Table 7. For Th_2Au^- , the VDE values are complicated by the similarity in the energies of the linear and C_{2v} isomers of the anion and by the fact that different spin states in the neutral have different overlaps with the geometry of the anion. Thus, we expect that the ${}^1\text{Th}_2\text{Au}^- (C_{2v})$ structure will give rise to transitions ranging from 1.41 to 1.55 eV, these encompassing the experimental with an intensity maximum EBE of 1.60 eV and an EBE onset at of 1.34 eV. The higher-energy C_{2v} spin states of the anion will give rise to lower VDE values. The linear ThThAu anion would have a VDE of 1.28 eV, this lying at the low intensity side of the observed EBE value. Thus, the results point to the observation of the C_{2v} structure as the dominant one in the EBE spectrum of Th_2Au for the first peak. It is possible that higher binding energies could involve electron detachment from the linear structure.

For Th_2AuO^- , there is a low-lying triplet state along with a singlet ground state for the C_{2v} structure. For the neutral, the optimized doublet and quartet states are essentially isoenergetic. The low-energy VDE is consistent with removal of an electron from the triplet to form either the doublet or quartet neutral with

Table 7. VDEs (eV) at the CCSD(T)/aT Level

anion	neutral	VDE
${}^1\text{Th}_2\text{Au}^- (C_{2v})$	${}^2\text{Th}_2\text{Au} (C_{2v})$	1.51
	${}^4\text{Th}_2\text{Au} (C_{2v})$	1.41
	${}^6\text{Th}_2\text{Au} (C_{2v})$	1.55
	${}^2\text{Th}_2\text{Au} (C_{2v})$	1.43
	${}^4\text{Th}_2\text{Au} (C_{2v})$	1.26
	${}^6\text{Th}_2\text{Au} (C_{2v})$	1.37
${}^5\text{Th}_2\text{Au}^- (C_{2v})$	${}^2\text{Th}_2\text{Au} (C_{2v})$	1.19
	${}^4\text{Th}_2\text{Au} (C_{2v})$	1.35
	${}^6\text{Th}_2\text{Au} (C_{2v})$	1.65
	${}^2\text{Th}_2\text{Au} (C_{\infty v})$	1.28
	${}^4\text{Th}_2\text{Au} (C_{\infty v})$	2.14
	${}^3\text{Th}_2\text{Au}^- (C_{\infty v})$	1.19 ^a
${}^1\text{Th}_2\text{Au}^- (C_{\infty v})$	${}^2\text{Th}_2\text{Au} (C_{\infty v})$	2.10 ^a
	${}^4\text{Th}_2\text{Au} (C_{\infty v})$	1.84
	${}^2\text{Th}_2\text{AuO} (C_{2v})$	1.87
	${}^3\text{Th}_2\text{AuO}^- (C_{2v})$	1.34
	${}^4\text{Th}_2\text{AuO} (C_{2v})$	1.39
	${}^2\text{Th}_2\text{O}_2^-$	0.68
${}^1\text{Th}_2\text{AuO}_2^- (C_s)$ (1)	${}^2\text{Th}_2\text{AuO}_2 (C_s)$ (1)	1.40 ^b
	${}^2\text{Th}_2\text{AuO}_2 (C_s)$ (2)	1.65
${}^2\text{ThO}_2^-$	${}^1\text{ThO}_2$	1.23
${}^3\text{AuO}_2^-$	${}^2\text{AuO}_2$	2.29
${}^3\text{ThAu}^-$	${}^2\text{ThAu}$	1.06
${}^1\text{ThAu}^-$	${}^4\text{ThAu}$	1.34
${}^5\text{ThAu}^-$	${}^2\text{ThAu}$	0.63
${}^4\text{ThAu}$	${}^4\text{ThAu}$	0.90
${}^2\text{ThO}^-$	${}^2\text{ThAu}$	0.51
${}^2\text{Th}_2\text{O}^- (C_{2v})$	${}^4\text{ThAu}$	0.78
${}^4\text{Th}_2\text{O}^- (C_{2v})$	${}^1\text{ThO}$	0.56
${}^1\text{AuO}^-$	${}^3\text{Th}_2\text{O} (C_{2v})$	1.37
${}^2\text{Th}_2^-$	${}^5\text{Th}_2\text{O} (C_{2v})$	1.38
${}^4\text{Th}_2^-$	${}^1\text{Th}_2\text{O} (C_{2v})$	1.56
${}^6\text{Th}_2^-$	${}^3\text{Th}_2\text{O} (C_{2v})$	1.29
${}^5\text{Th}_2\text{O} (C_{2v})$	${}^5\text{Th}_2\text{O} (C_{2v})$	1.23
${}^1\text{Th}_2\text{O} (C_{2v})$	${}^1\text{Th}_2\text{O} (C_{2v})$	1.48
${}^2\text{AuO}$	${}^2\text{AuO}$	2.29
${}^3\text{Th}_2$	${}^3\text{Th}_2$	0.77
${}^1\text{Th}_2$	${}^1\text{Th}_2$	0.80
${}^5\text{Th}_2$	${}^5\text{Th}_2$	1.34
${}^3\text{Th}_2$	${}^3\text{Th}_2$	0.61
${}^1\text{Th}_2$	${}^1\text{Th}_2$	0.64
${}^5\text{Th}_2$	${}^5\text{Th}_2$	1.17
${}^3\text{Th}_2$	${}^3\text{Th}_2$	0.81
${}^1\text{Th}_2$	${}^1\text{Th}_2$	0.79
${}^5\text{Th}_2$	${}^5\text{Th}_2$	1.20

^aaD basis set. ^b1.42 eV with the awT basis set.

respective VDE values of 1.34 and 1.39 eV in comparison with the experimental EBE peak value of 1.59 eV and an EBE onset of 1.30 eV. The higher-energy EBE band is consistent with a transition from the ground state singlet to the doublet and quartet neutral states with calculated values of 1.84 and 1.89 eV; these predicted values fall in the middle of the experimental EBE range of 1.85–2.05 eV.

For ${}^1\text{Th}_2\text{AuO}_2^- (C_s)$ (1), the higher-energy ${}^1\text{Th}_2\text{AuO}_2^- (C_s)$ (2) structure with the O atom bridging two Th atoms is 4 kcal/mol higher in energy and may be present in the experiment. The

Table 8. Heats of formation and BDEs in kcal/mol at 0 K

molecule	$\Delta H_{f,0K}$	$\Delta H_{f,298K}$	BDE		
			Th–Au	Th–Th	M–O
² ThAu	162.5	162.4	69.4		
³ ThAu ⁻	139.2	139.1	39.5 Th + Au ⁻		
² Th ₂ Au (C_{2v})	227.2	227.1	81.4 Th ₂ + Au	79.2 ThAu + Th	
² Th ₂ Au ($C_{\infty v}$)	226.6	226.7	82.0 Th ₂ + Au	79.8 ThAu + Th	
¹ Th ₂ Au ⁻ (C_{2v})	197.5	197.4	58.6 Th ₂ + Au ⁻	85.6 ThAu ⁻ + Th	
¹ Th ₂ Au ⁻ ($C_{\infty v}$)	198.2	198.3	57.2 Th ₂ + Au ⁻	84.9 ThAu ⁻ + Th	
² Th ₂ AuO (C_{2v})	80.2	79.7	93.9 Th ₂ O + Au	75.4 ThAuO + Th	141.3 Th ₂ Au + O
¹ Th ₂ AuO ⁻ (C_{2v})	46.8	46.5	74.1 Th ₂ O + Au ⁻	74.4 ThAuO ⁻ + Th	209.7 Th ₂ Au ⁻ + O
² Th ₂ AuO ₂ (C_s) (1) ^a	-74.6	-75.3	77.5 Th ₂ O ₂ + Au	171.3 ThAuO ₂ + Th	213.8 Th ₂ AuO + O
¹ Th ₂ AuO ₂ ⁻ (C_s) (1)	-103.4	-104.1	53.1 Th ₂ O ₂ + Au ⁻	118.3 ThAuO ₂ ⁻ + Th	209.2 Th ₂ AuO ⁻ + O
² ThAuO (C_s)	11.7	11.4	68.3 ThO + Au		209.8 ThAu + O
¹ ThAuO ⁻ (C_s)	-22.7	-23.0	90.3 ThO ⁻ + Au		211.0 ThAu + O ⁻
² ThAuO ₂ (C_1)	-47.1	-47.6	26.9 ThO ₂ + Au		117.8 ThAuO + O
¹ ThAuO ₂ ⁻ (C_{2v})	-129.0	-129.3	55.6 ThO ₂ + Au ⁻		166.5 ThAuO + O ⁻
³ Th ₂ O (C_{2v})	86.1	85.6		49.8 ThO + Th	
² Th ₂ O ⁻ (C_{2v})	55.2	54.7		67.3 ThO + Th ⁻	
¹ Th ₂ O ₂ (C_{2h})	-85.1	-86.1			230.2 Th ₂ O + O
² Th ₂ O ₂ ⁻ (C_{2v})	-96.3	-97.3			208.2 Th ₂ O + O ⁻
² AuO	99.1	99.0			47.9
¹ AuO ⁻	43.7	43.5			50.1 Au ⁻ + O
² AuO ₂ ($D_{\infty h}$)	88.6	88.1			69.5 AuO + O
³ AuO ₂ ⁻ ($D_{\infty h}$)	7.2	6.7			95.5 AuO ⁻ + O
¹ ThO	-8.0	-8.3			210.9
² ThO ⁻	-20.2	-20.4			189.9 Th + O ⁻
¹ ThO ₂ (C_{2v})	-108.2	-108.7			159.2 ThO + O
² ThO ₂ ⁻ (C_{2v})	-135.6	-136.1			153.4 ThO + O ⁻
³ Th ₂	220.7	220.5		67.2	
² Th ₂ ⁻	202.9	202.8		71.4	

^aCalculated using EAs and the heats of formation of the anion, ¹Th₂AuO₂⁻ (C_s) (1).

calculated VDE value is 1.40 eV without the outer core electrons correlated and 1.42 eV with the outer core electrons correlated for ¹Th₂AuO₂⁻ (C_s) (1). The VDE value for the higher-energy anion structure ¹Th₂AuO₂⁻ (C_s) (2) is 1.65 eV. These calculated VDE values fall under the band in the experimental EBE spectrum centered at 1.56 eV.

For Th₂O⁻, the quartet state is slightly higher in energy than the doublet. The ground state of the Th₂O neutral can be either the triplet or the quintet. The calculated VDE values for the triplet and quintet states are essentially the same and in good agreement with the experimental EBE values with an EBE onset at 1.30 eV and a maximum intensity in the EBE peak at 1.49 eV.

Heats of Formation and BDEs. Calculated heats of formation and selected BDEs are reported in Table 8, and compared with the experimental values when available. The experimental heat of formation of ThO has been reported as -5.0 ± 2.4 ⁷⁰ and -6.4 ± 3.3 kcal/mol.⁵⁶ In comparison with these, our calculated value is more negative ($\Delta H_{f,298K} = -8.3$ kcal/mol) and falls essentially within the experimental error bars. The experimental heat of formation of ThO₂ has been reported as -108.8 ± 3.0 ⁷⁰ and -104.8 ± 10 kcal/mol⁵⁶ and our calculated value ($\Delta H_{f,298K} = -108.7$ kcal/mol) is in excellent agreement with these values. The experimental heat of formation of Th₂ has been reported to be 217.0 and 216.2 ± 5.8 (0 K) kcal/mol⁵⁶ and our calculated heat of formation, $\Delta H_{f,298K} = 220.5$ kcal/mol, is slightly more positive and within the reported experimental error bars. For the remaining molecules for which the experimental data are not

available, the current values represent the best available thermodynamic data. Spin-orbit effects for the atoms were included in the calculations of the heats of formation but not for the molecules. Such molecular spin-orbit effects have been found⁷¹ to be small in calculations of the heats of formation of ThF₄ and ThCl₄ (~ 0.2 kcal/mol) and were not included. The good agreement with the available values for the heats of formation suggests that these molecular spin-orbit corrections are not large. In addition, the good agreement between the calculated and experimental values for the EAs shows that spin-orbit effects are cancelling each other for these quantities.

BDEs are valuable parameters for understanding the bonding in these species. The BDE of AuO has been reported to be 53.3 ± 5 kcal/mol, whereas our calculated value of 48 kcal/mol is slightly smaller than that, it is likely to be more reliable.⁵³ Roos et al.⁶ report a CASPT2 BDE for Th₂ of 3.28 eV (75.6 kcal/mol), which is 8 kcal/mol larger than our value, but is not consistent with the experimental heats of formation.

The BDE values of diatomic ThAu and Th₂ are very similar to one another, with the BDE value of ThAu being 2 kcal/mol larger. At 211 kcal/mol, the BDE value of the ThO diatomic is much larger, whereas at 48 kcal/mol, the BDE of AuO is much smaller, suggesting that ThO bonds will govern over AuO bonds in the structures that are formed.

For Th₂Au, we find that the C_{2v} and $C_{\infty v}$ ThThAu isomers have comparable energies, which is consistent with the similar BDE values for Th–Th and Th–Au. The Th–Th and Th–Au

BDE values in the Th₂Au cluster are larger than in the diatomics, so there might be some metallic character in the trimer. This is consistent with the Th–Th bond distances ranging only from 2.71 to 2.76 Å in the structures and in diatomic Th₂. By contrast, the ThAu bond distances in the trimer species are significantly longer than in diatomic ThAu. It is also important to note that the Th–Th interaction is key to the stability of the species, as the $D_{\infty h}$ ThAuTh species is much higher in energy. In this $D_{\infty h}$ structure, there can be no overlap of the Th 6d orbitals with each other. The only bonding utilizes the valence s-orbitals, leading to a total BO of 0.5, was caused by placing five electrons into the three valence s-orbitals, that is, a bonding orbital, a nonbonding orbital, and an antibonding orbital.

Although the first Th–O BDE in Th₂O is only 50 kcal/mol, the second Th–O BDE is much higher. In contrast, the ThO BDE in ThO₂ is 159 kcal/mol. The AuO BDE is much smaller, at 48 kcal/mol. The large Th–O BDE and the lower AuO BDE mean that Th₂O and Th₂O₂ can be considered as core structural units. This is consistent with the relative energies of the isomers discussed above, where the Au is best described as complexing to Th₂O or to Th₂O₂. There is still a significant interaction of Au with the cluster with a binding energy of 88 kcal/mol for Th₂AuO where Au can bridge the two Th atoms connected by an oxygen. This Au-cluster interaction decreases by 20 kcal/mol when Au can only bind to a Th or bridge across the Th₂O₂ cluster as in Th₂AuO₂. The binding of Au[−] to the cluster is about 20 kcal/mol smaller for Th₂O and Th₂O₂. Note that the Th-cluster BDE in Th₂AuO₂ is quite high because of breaking two Th–O bonds when Th is liberated. Note also that when Th is removed, the oxygen binding energy to the cluster is substantially decreased, again consistent with the conclusion that the ThO bonds are controlling the energetics of cluster formation.

Bonding. The BOs for the Th–Th bonds are calculated based on analyses of the MOs and of the NBOs. The values are reported in Table 5 and the orbital diagrams are shown in the Supporting Information. We first discuss the bonding in the core fragments.

Th₂. The bonding of the clusters containing Au can be best described by first examining the structures containing Th and O. ³Th₂ has the electron configuration $(7s\sigma_g)^2(6d\delta_g)^1(6d\sigma_g)^1(6d\pi_u)^4$, consistent with a BO of 4.0 as noted by Roos et al.⁶ The electron configuration for the corresponding ¹Th₂ is $(7s\sigma)^2(6d\sigma)^2(6d\pi)^4$ with a BO of 4.0 as well. From the NBO analysis, the lowest energy ³Th₂, with two unpaired electrons in d δ and d σ , has two bonds formed by only d orbitals, while the other two bonds possess both mixed d- and s-orbital characters. For ²Th₂[−], the BO calculated using an analysis of the MOs is 3.5 with an electron configuration of $(7s\sigma)^2(6d\delta)^1(6d\pi)^4$. There is also a $(6d\pi)^2$ nonbonding lone pair. From the NBO analysis, the BO should be 4.5 with two bonds, having mostly d character and with the other 2.5 bonds exhibiting mixed d- and s-characters. The slightly higher in energy isomers, ⁶Th₂[−] and ⁴Th₂[−], should have BOs of 4.0 from MO analysis, with the electronic configurations $(7s\sigma)^2(6d\sigma)^1(6d\delta)^1(6d\delta)^1(6d\pi)^3(6d\pi$ lone pair)¹ and $(7s\sigma)^2(6d\sigma)^1(6d\delta)^1(6d\pi)^4(6d\pi$ lone pair)¹, respectively. From the NBO analysis, ⁶Th₂[−] and ⁴Th₂[−] have BOs of 3.5 and 4.5, respectively.

Th Oxygen Clusters. Th₂O can be envisioned as being held together by ionic bonding between an O^{2−} and two Th⁺ ions, consistent with a ground state triplet with a $(7s\sigma)^2(6d\delta)^1(6d\pi)^1$ configuration and a $(6d\pi)^2$ lone pair, resulting in a BO of 2.0.

(We use the same labels for describing the types of bonding as in the linear Th₂ configuration, although these are not the correct symmetry labels in lower symmetry.) ⁵Th₂O and ¹Th₂O have a BO of 2.0 as well based on an analysis of the MOs. The quintet has a $(7s\sigma)^2(6d\pi)^1(6d\delta)^1$ configuration with two $(6d\pi, 6d\delta)$ unpaired lone pair electrons and the singlet has a $(7s\sigma)^2(6d\pi)^2$ configuration with a $(6d\pi)^2$ lone pair. The NBO analysis gives a different BO of only 0.5 for the Th–Th bond. The Th–O “bonds” in all three neutral electronic states have a BO of 1.96 from the NBO analysis; these Th–O bonds are mostly localized on the O atom. The O atom has a charge of ca. −1.5 lel, confirming the ionic character of the Th–O bond. ²Th₂O[−] has an extra $(6d\pi)$ electron and ⁴Th₂O[−] has an extra $(6d\delta)$ lone pair electron with resulting BOs of 2.5 and 1.5, respectively. Th₂O can be considered as an ionically bonded species built on O^{2−} and Th⁺ ions because the charge on the O atom remains the same; the Th–O bonds are again localized mostly on the O atom.

Th₂O₂ can be envisioned as an ionically bonded species with two Th²⁺ and two O^{2−}. There is no Th–Th bonding in this case, but there is a lone pair on each Th atom consistent with a nonbonding $(6d\pi)^4$ configuration and with loss of the 7s electrons to form the +II formal oxidation state. Th₂O₂[−] can also be considered as being held together by ionic bonding with two O^{2−} ions and with a Th⁺ ion and a Th²⁺ ion. As with the neutral, there is no Th–Th bonding, and there is a lone pair on each Th atom with a nonbonding $(6d\pi)^4$ and an extra electron lone pair on one of Th atoms. From the NBO analysis, the O atoms' charges remain unchanged at ca. −1.5 lel for both the neutral and the anion; the Th–O “bonds” are highly polarized, with most of the electron density being mostly localized on the O atom.

Th₂Au. It is possible to describe Th₂Au with an ionic model as Au[−](Th₂)⁺. The Au atom has a high EA and could abstract an electron from the Th₂ moiety. The Th₂ bond in C_{2v} Th₂Au would then be $(7s\sigma)^2(6d\delta)^1(6d\pi)^4$, resulting in a BO of 3.5, based on the MO analysis. ²Th₂Au (C_{∞v}) has an $(7s\sigma)^2(6d\sigma)^1(6d\pi)^4$ electronic configuration with a BO of 3.5, based on the MO analysis, where the unpaired electron resides in a 6d σ orbital, which is different from the C_{2v} isomer, where the unpaired electron is a 6d δ . ²Th₂⁺ has the electronic configuration, $(7s\sigma)^2(6d\sigma)^1(6d\pi)^4$, so the linear conformer has the same electron configuration for the Th–Th bond.

In the simple ionic model, the anion Th₂Au[−] should have the Th₂ MO scheme of $(7s\sigma_g)^2(6d\delta_g)^1(6d\sigma_g)^1(6d\pi_u)^4$ for neutral ³Th₂ or the MO scheme $(7s\sigma)^2(6d\sigma)^2(6d\pi)^4$ for the ¹Th₂ configuration as the singlet Th₂ is just 0.5 kcal/mol higher in energy; the Th–Th BO would thus equal 4.0. In fact, the linear structure of singlet ThThAu[−] does have the bonding pattern of the singlet. Note that the ³Th₂Au[−], which would give the ionic species, (³Th₂) (Au[−]), is 2.3 kcal/mol higher in energy at the CCSD(T)/aT level of theory. However, the Th–Au bonds in Th₂Au[−] C_{2v} structure are more elongated by the additional electron repulsion from Au[−] than in the linear anion. For Th₂Au[−] C_{2v}, the bonding is best described as $(7s\sigma_g)^2(6d\pi_u)^4$, with a nonbonding orbital composed of lone pairs on the Th atom, giving a Th–Th BO of 3.0.

The NBO analysis for ¹Th₂Au[−] (C_{2v}) has a Th–Th BO of 1.92, with the Th 6d orbitals as the main contributors. Linear, C_{∞v}, ¹Th₂Au[−] has a Th–Th BO of 2.92 with a shorter Th–Th bond than the C_{2v} isomer. Two of the Th–Th bonds are shared about equally by both Th atoms through their 6d orbitals, and the third bond is more localized on the Th atom, which is directly bonded to the Au atom through a mixture of s–d

orbitals. ${}^2\text{Th}_2\text{Au}$ ($C_{\infty v}$) has a Th–Th BO of 2.93 as well. The unpaired α spin is mostly on the Th atom (0.74 e) that is not bound to the Au atom, with the remaining spin (0.26 e) on the Th atom that binds the Au atom. ${}^2\text{Th}_2\text{Au}$ (C_{2v}) is predicted to have a BO, which is artificially high because of the presence of open shells (different α and β spins) and the presence of multicentered bonds.

Th₂AuO_{1–2}. In the simple ionic model, the addition of an Au atom to Th_2O would generate an Au^- ion and a ${}^2\text{Th}_2\text{O}^+$ ion. ${}^2\text{Th}_2\text{O}^+$ is generated by the removal of an electron from the neutral ${}^3\text{Th}_2\text{O}$'s lone pair electron on the Th atoms to give a $(7s\sigma)^2(6d\delta)^1(6d\pi)^2$ configuration. The Th–Th BO for ${}^2\text{Th}_2\text{O}^+$ as well as for ${}^2\text{Th}_2\text{AuO}$ of 2.5 does not change from that in ${}^3\text{Th}_2\text{O}$. The slightly higher-energy ${}^4\text{Th}_2\text{AuO}$ is described as $({}^4\text{Th}_2\text{O})^+\text{Au}^-$, with a configuration of $(7s\sigma)^2(6d\delta)^1(6d\pi)^1$ and with a $(6d\pi)^1$ lone pair configuration, resulting in a BO of 2.0. Addition of the electron as part of a lone pair to form ${}^1\text{Th}_2\text{AuO}^-$ adds enough electron repulsion to elongate the Th–Th bond relative to the neutral, so that there are then two lone pairs and a Th–Th π -bond with a BO of 1.0. This Th–Th bond in ${}^1\text{Th}_2\text{AuO}^-$, which can be considered as $({}^1\text{Th}_2\text{O})\text{Au}^-$, is 0.08 Å longer than in ${}^1\text{Th}_2\text{O}$, with a BO of 2.0. In ${}^1\text{Th}_2\text{O}$, there is a $(6d\pi)^2$ lone pair and a $(7s\sigma)^2(6d\pi)^2$ configuration for the Th–Th interaction. The Th–Th bond distance for the higher-energy anion, ${}^3\text{Th}_2\text{AuO}^-$, is much closer to the Th–Th bond distance of the neutral structure; moreover, ${}^3\text{Th}_2\text{AuO}^-$ has a BO of 2.5 with $(7s\sigma)^2(6d\pi)^3$ and a $(6d\pi)^1$ lone pair electronic configuration. The ${}^3\text{Th}_2\text{O}$ ground state with a Th–Th bond is 0.35 Å longer than the Th–Th bond in ${}^3\text{Th}_2\text{AuO}^-$ and has a $(7s\sigma)^2(6d\delta)^1(6d\pi)^1$ configuration with a $(6d\pi)^2$ lone pair and a BO of 2.0.

From the NBO analysis, the lowest energy neutral, ${}^2\text{Th}_2\text{AuO}$, and the anion, ${}^1\text{Th}_2\text{AuO}^-$, have the same BOs of 2.48 and 0.97 as found from the MO analysis (2.5 and 1.0, respectively) given above. In addition, the NBO analysis shows a 3 center-2 electron (3c-2e) AuThTh bond for both the lowest energy Th_2AuO neutral and anion structures. This 3c-2e bond is a s–d bond with the most contribution from the Au atom's s-orbitals and can be explained by an Au atom contribution to the Th–Th π bonds from the MO analysis. Also, the NBO analysis confirms that the unpaired electron is mostly $6d\delta$ and is equally shared by both Th atoms. The Th–O bonds in these Th_2AuO molecules are highly polarized. The charges on O and Au atoms of *ca.* –0.5 lel and *ca.* –1.5 lel, respectively, remain almost unchanged for the Th_2AuO neutral and anion and are the same as for the Th_2Au and Th_2O molecules, respectively.

Addition of an Au atom to Th_2O_2 abstracts a lone pair electron from the Th atom to generate $\text{Au}^-(\text{Th}_2\text{O}_2)^+$. As there is no Th–Th bond in Th_2O_2 , there is not one in Th_2AuO_2 . The location of the Au atom on one of the Th atoms is consistent with the formation of this ionic bonded structure. The addition of an electron to form $(\text{Th}_2\text{O}_2)\text{Au}^-$ replaces the lone pair on the Th atom and the Au atom does not change its position. Note that in all cases, there are a number of low-lying isomers consistent with the lack of directional bonding in an ion pair. The similarity in the EAs is also consistent with the ion pair-bonding model because the removal of an electron is from a lone pair on the Th atoms in Th_2AuO^- and $\text{Th}_2\text{AuO}_2^-$ or from a higher-energy Th–Th bonding orbital in Th_2Au^- .

CONCLUSIONS

Anion photoelectron spectroscopy of Th_2O^- , Th_2Au^- , and $\text{Th}_2\text{AuO}_{1,2}^-$ yielded VDE in the range of 1–2 eV. Correlated MO theory calculations at the CCSD(T) level gave values that are consistent with the experimental data and showed that in many cases there are close-lying anion and neutral clusters with different geometries and spin states that can account for the observed spectra. The calculations are in agreement with the VDEs within 0.10 eV. The results suggest that there is a wealth of information for even such simple triatomic through pentatomic species.

A plot of the Th–Th BOs from an analysis of the MOs versus Th–Th bond distances is shown in Figure 4 (the corresponding

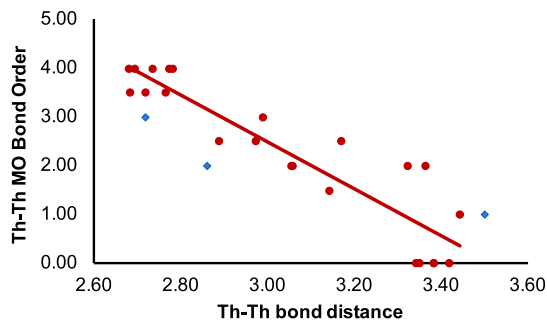


Figure 4. Trendline in Th–Th BO from MO analysis vs the Th–Th bond distance in Å. Blue diamonds represent Pyykkö's values⁷² from covalent bond radii and are not part of the trendline.

results for the BO from the NBOs are given in the Supporting Information). We focus on the Th–Th bonds as the highly polarized Th–O and Th–Au bonds and their BOs do not change as significantly with the bond distance. The Th–Th bond distances range from about 2.7 to 3.5 Å and the BOs range from 4 to 0. There is a qualitative trend of a decrease in BO with an increasing bond distance, but it is interesting to note that there can be a significant difference in the BO for a given distance especially for longer distances. The relationship between BOs from the MOs and bond distances is reasonably consistent with the bond distances derived from Pyykkö's covalent radii⁷² for Th of 3.50 Å for a Th–Th single bond, 2.86 Å for a Th–Th double bond, and 2.72 Å for a Th–Th triple bond, where these radii are derived for different atoms interacting with Th.

We find that a simple ionic model provides insights into the bonding in these species because of the large EA of Au, the strong Th–O bond, the weak AuO bond, and the low ionization potentials (IPs) of the $\text{Th}_2\text{O}_{0,1,2}$ clusters. The EA of Au is 2.3 eV and the IPs of Th₂, Th_2O , and Th_2O_2 are 4.90, 5.04, and 5.42 eV calculated at the CCSD(T)/awT level. Thus, the difference in the IP-EA that needs to be overcome by an attractive ionic interaction ranges from 2.6 to 3.1 eV. A simple Coulombic model with Au^- at a distance of 3.0 Å (an approximate average of the Th–Au distances) from the positive charge gives 4.8 eV in terms of the Coulombic interaction, so there is a sufficient Coulombic attraction energy for these charge transfer processes to occur leading to ion pair formation. As shown by the values in Table 8, the ionic component contributes a significant amount to the BDEs. Even ThAu can have a significant ionic component as the IP of Th is 6.31 eV⁷³ and the ThAu distance is 2.70 Å (see Supporting Information). In this case, the Coulombic attraction energy is 5.3 eV and the IP-EA difference is 4.0 eV so the

Coulombic bond energy is 1.3 eV out of the total BDE of 3.0 eV (Table 8). We note that ThAu_4 has been predicted to have 4 Au^- ligands bonded to Th⁷⁴ and that Pyykkö has summarized work on cesium auride, Cs^+Au^- , as well as many other unique properties of Au in terms of its bonding, especially in terms of its large electronegativity.^{75–77}

The neutral Th_2Au structure is quite flexible as would be expected of a species with a closed shell Au^- bonded to a Th_2^+ core with a strong Th–Th bond in the ionic model. The Au^- can then effectively move around the Th_2^+ core with low barriers. Although the analysis of the BDEs and bond distances in Th_2Au relative to the diatomics Th_2 and ThAu suggested possible metallic character in these species, we prefer the ionic model for the bonding rather than a metal–metal bonding model as would be appropriate for Au_3 , which exhibits similar flexibility but for a different reason.⁷⁸ The anion is prepared by adding the electron to the Th_2^+ core. There are a number of low-lying spin states when only the metals are present because of the different ways of coupling the spins in $\text{Th}_2^{+/-}$ as Au^- is a closed shell in the neutral and in the anion. Thus, the Th–Th BO is dominated by what happens in the diatomic $\text{Th}_2^{+/-}$ moiety. The interaction of the Au^- with the $\text{Th}_2^{+/-}$ group can impact the Th–Th bond distances; for example, the Th–Th bond distance lengthens in the C_{2v} neutral structure because of electron repulsion from Au^- with both Th atoms.

In the presence of oxygen, the energetics are dominated by the presence of strong Th–O bonds as the Au–O bond is quite weak. The Th–O interactions have a dominant ionic component and we treat O as a formal O^{2-} . Thus, for Th_2O , we would expect to have two Th(I), each of which has a ground state $7s^26d^1$ electron configuration; the $7s^16d^2$ and $7s^25f^1$ excited states of the ion are not that high in energy.⁷³ Thus, we expect a number of low-lying spin states for Th_2O as is predicted. In addition, the ThOTh bond angle is quite flexible ranging from 90 to 110° depending on the spin state. The Th–Th bond is longer than in $\text{Th}_2\text{Au}^{0/-}$ ranging from 3.0 to 3.4 Å depending on the spin state but is still substantially less than twice the atomic radius of 1.80 Å.⁷⁹ Thus, there is always some metal–metal Th bonding present in these Th clusters held together by a single O atom. Addition of an electron to Th_2O tends to make the Th–Th bond distances about the same, near 3.20 Å. The Th–Th BO in Th_2O is 2.0 in the neutral and 1.5 to 2.5 in the anion depending on the spin state. The addition of Au to Th_2O can be described as a charge transfer process leading to the formation of the $[\text{Th}_2\text{O}^+][\text{Au}^-]$ ion pair because of the large EA of Au and the modest IP of Th_2O . The Th–Th bond length shortens on addition of the Au consistent with the ionic model. The addition of the electron to form Th_2AuO^- leads to Au^- bonded to a neutral ThOTh unit as the additional negative charge goes onto the metal oxide. Although the energy differences between the singlet and triplet states are small in Th_2AuO^- , the Th–Th bond distance has a surprisingly large variation with the longer bond distance by 0.4 Å corresponding to the more stable species with a BO of 1.0. The triplet has a BO of 2.5. Again, there is a balance in the electron repulsion so that the singlet minimizes electron repulsion by the formation of lone pairs on Th.

The bonding in Th_2O_2 is dominated by the ion pairing of the two O^{2-} with the two Th(II). The Th–Th bond distance is still between 3.3 and 3.4 Å, and in principle, could retain some metal–metal character. However, in this case, the electrons that are on Th localize as lone pairs and it is best to describe Th_2O_2 as not having a metal–metal bond. Addition of Au to Th_2O_2 again leads to the formation of an ion pair $[\text{Th}_2\text{O}_2^+][\text{Au}^-]$ and the

Th–Th distance does not significantly change on addition of Au. This is consistent with the charge of +2 on the metal.

Overall, the results show that what one might consider as a cluster with metal–metal bonds between Th and Au may have a significant ionic component to the bonding and that an ion pair model can account for the MOs. The results show, in the presence of moieties with moderately large EAs such as Au and moderate ionization potentials such as the Th species, that one cannot ignore the possibility of significant ionic character even for interactions between metals. As a metal, Au with its quite high EA may prove to have unique interactions and serve as a different type of probe for the properties of the metal and metal oxide clusters. The results also suggest that one must go beyond just using the bond distance to obtain the BO to describe the types of bonding that are present in these thorium metal clusters and oxides.

ASSOCIATED CONTENT

Supporting Information

The Supporting Information is available free of charge at <https://pubs.acs.org/doi/10.1021/acs.jpca.0c09766>.

Complete citations for refs;^{31,40,61} additional relative energies and geometry parameters at different levels of theory for all isomers and their spin states; total energies in atomic units; components for calculating the total atomization energies and calculated heats of formation in kcal/mol; adiabatic EAs (eV) (ΔH_{0K}) at the B3LYP/aD level; ionization potentials of Th_2 , Th_2O , and Th_2O_2 in eV at 0 K. NBO BOs versus bond distances in angstroms; trendlines in Th–Th BO from NBO and MO analysis versus the Th–Th bond distance; and isomeric structures, MOs, and XYZ optimized coordinates for the larger molecules ([PDF](#))

AUTHOR INFORMATION

Corresponding Authors

Kit H. Bowen – Department of Chemistry, Johns Hopkins University, Baltimore, Maryland 21218, United States; orcid.org/0000-0002-2858-6352; Email: kbowen@jhu.edu

David A. Dixon – Department of Chemistry and Biochemistry, University of Alabama, Tuscaloosa, Alabama 35401, United States; orcid.org/0000-0002-9492-0056; Email: dadixon@ua.edu

Authors

Zhaoguo Zhu – Department of Chemistry, Johns Hopkins University, Baltimore, Maryland 21218, United States

Mary Marshall – Department of Chemistry, Johns Hopkins University, Baltimore, Maryland 21218, United States

Rachel M. Harris – Department of Chemistry, Johns Hopkins University, Baltimore, Maryland 21218, United States

Monica Vasiliu – Department of Chemistry and Biochemistry, University of Alabama, Tuscaloosa, Alabama 35401, United States

Complete contact information is available at:

<https://pubs.acs.org/10.1021/acs.jpca.0c09766>

Notes

The authors declare no competing financial interest.

ACKNOWLEDGMENTS

The experimental portion of this material is based upon work supported by the U. S. Department of Energy (DOE), Office of Science, Office of Basic Energy Sciences, Heavy Element Chemistry program under Award Number DE-SC0019317 (K.H.B.). The computational portion of this material is based upon work supported by the U. S. Department of Energy (DOE), Office of Science, Office of Basic Energy Sciences, Heavy Element Chemistry program under Award Number DE-SC0018921 (D.A.D.). D.A.D. also thanks the Robert Ramsay Fund at The University of Alabama.

REFERENCES

- (1) Kelley, M. P.; Popov, I. A.; Jung, J.; Batista, E. R.; Yang, P. δ and φ Back-Donation in AnIV Metallacycles. *Nat. Commun.* **2020**, *11*, 1558.
- (2) Denning, R. G. Electronic Structure and Bonding in Actinyl Ions. *Complexes, Clusters and Crystal Chemistry; Structure and Bonding*; Springer, 1992; Vol. 79, pp 215–276.
- (3) Denning, R. G. Electronic Structure and Bonding in Actinyl Ions and Their Analogs. *J. Phys. Chem. A* **2007**, *111*, 4125–4143.
- (4) Hu, H.-S.; Kaltsoyannis, N. The Shortest Th-Th Distance from a New Type of Quadruple Bond. *Phys. Chem. Chem. Phys.* **2017**, *19*, 5070–5076.
- (5) Souter, P. F.; Kushto, G. P.; Andrews, L.; Neurock, M. Experimental and Theoretical Evidence for the Formation of Several Uranium Hydride Molecules. *J. Am. Chem. Soc.* **1997**, *119*, 1682–1687.
- (6) Roos, B. O.; Malmqvist, P.-Å.; Gagliardi, L. Exploring the Actinide–Actinide Bond: Theoretical Studies of the Chemical Bond in Ac₂, Th₂, Pa₂, and U₂. *J. Am. Chem. Soc.* **2006**, *128*, 17000–17006.
- (7) Knecht, S.; Jensen, H. J. A.; Sauv, T. Relativistic quantum chemical calculations show that the uranium molecule U₂ has a quadruple bond. *Nat. Chem.* **2019**, *11*, 40–44.
- (8) Straka, M.; Pyykkö, P. Linear HThThH: A Candidate for a Th–Th Triple Bond. *J. Am. Chem. Soc.* **2005**, *127*, 13090–13091.
- (9) Zhou, J.; Sonnenberg, J. L.; Schlegel, H. B. Theoretical Studies of AnII₂(C₈H₈)₂(An = Th, Pa, U, and Np) Complexes: The Search for Double-Stuffed Actinide Metalloccenes. *Inorg. Chem.* **2010**, *49*, 6545–6551.
- (10) Wang, C.-Z.; Gibson, J. K.; Lan, J.-H.; Wu, Q.-Y.; Zhao, Y.-L.; Li, J.; Chai, Z.-F.; Shi, W.-Q. Actinide (An = Th–Pu) dimetallocenes: promising candidates for metal–metal multiple bonds. *Dalton Trans.* **2015**, *44*, 17045–17053.
- (11) Ge, X.; Dai, X.; Zhou, H.; Yang, Z.; Zhou, R. Stabilization of Open-Shell Single Bonds within Endohedral Metallofullerene. *Inorg. Chem.* **2020**, *59*, 3606–3618.
- (12) Andrews, L.; Gong, Y.; Liang, B.; Jackson, V. E.; Flamerich, R.; Li, S.; Dixon, D. A. Matrix Infrared Spectra and Theoretical Studies of Thorium Oxide Species: ThO_x and Th₂O_y. *J. Phys. Chem. A* **2011**, *115*, 14407–14416.
- (13) Heaven, M. C.; Barker, B. J.; Antonov, I. O. Spectroscopy and Structure of the Simplest Actinide Bonds. *J. Phys. Chem. A* **2014**, *118*, 10867–10881.
- (14) Steinle, T.; Kokkin, D. L.; Muscarella, S.; Ma, T. Detection of the Thorium Dimer via Two-Dimensional Fluorescence Spectroscopy. *J. Phys. Chem. A* **2015**, *119*, 9281–9285.
- (15) Sculford, S.; Braunstein, P. Intramolecular d10-d10 interactions in heterometallic clusters of the transition metals. *Chem. Soc. Rev.* **2011**, *40*, 2741–2760.
- (16) Baruah, T.; Blundell, S. A.; Zope, R. R. Electronic and Structural Properties of Small Clusters of Na_nAu and Na_nAg (n = 1 – 10). *Phys. Rev. A: At., Mol., Opt. Phys.* **2001**, *64*, 043202.
- (17) Britto Hurtado, R.; Cortez-Valadez, M.; Gámez-Corralles, R.; Flores-Acosta, M. Structural and Vibrational Properties of Gold-Doped Titanium Clusters: A First-Principles Study. *Comput. Theor. Chem.* **2018**, *1124*, 32–38.
- (18) Lu, P.; Liu, G.-H.; Kuang, X.-Y. Probing the Structural and Electronic Properties of Bimetallic Chromium-Gold Clusters Cr_mAu_n ($m + n \leq 6$): Comparison with Pure Chromium and Gold Clusters. *J. Mol. Model.* **2014**, *20*, 2385.
- (19) Bishea, G. A.; Arrington, C. A.; Behm, J. M.; Morse, M. D. Resonant two-photon ionization spectroscopy of coinage metal trimers: Cu₂Ag, Cu₂Au, and CuAgAu. *J. Chem. Phys.* **1991**, *95*, 8765–8778.
- (20) Bonačić-Koutecký, V.; Burda, J.; Mitić, R.; Ge, M.; Zampella, G.; Fantucci, P. Density Functional Study of Structural and Electronic Properties of Bimetallic Silver-Gold Clusters: Comparison with Pure Gold and Silver Clusters. *J. Chem. Phys.* **2002**, *117*, 3120–3131.
- (21) Yuan, H. K.; Kuang, A. L.; Tian, C. L.; Chen, H. Structural and electronic properties of Au_n-xPtx (n = 2–14; x ≤ n) clusters: The density functional theory investigation. *AIP Adv.* **2014**, *4*, 037107.
- (22) Zhang, H.-R.; Zhao, Y.-R.; Gao, R.; Hu, Y.-F. Insights into the structures, stabilities, electronic and magnetic properties of X₂Aun (X = La, Y, and Sc; n = 1–9) clusters: comparison with pure gold clusters. *Mol. Phys.* **2017**, *115*, 308–319.
- (23) Gerhards, M.; Thomas, O. C.; Nilles, J. M.; Zheng, W.-J.; Bowen, K. H. Cobalt-Benzene Cluster Anions: Mass Spectrometry and Negative Ion Photoelectron Spectroscopy. *J. Chem. Phys.* **2002**, *116*, 10247–10252.
- (24) Ho, J.; Ervin, K. M.; Lineberger, W. C. Photoelectron spectroscopy of metal cluster anions: Cu-n, Ag-n, and Au-n. *J. Chem. Phys.* **1990**, *93*, 6987–7002.
- (25) Burkart, S.; Blessing, N.; Klipp, B.; Müller, J.; Ganteför, G.; Seifert, G. Experimental verification of the high stability of Al13H: a building block of a new type of cluster material? *Chem. Phys. Lett.* **1999**, *301*, 546–550.
- (26) Siekmann, H. R.; Lüder, C.; Faehrmann, J.; Lutz, H. O.; Meiwe-Broer, K. H. The Pulsed Arc Cluster Ion Source (PACIS). *Z. Phys. D: At., Mol. Clusters* **1991**, *20*, 417–420.
- (27) Zhang, X.; Wang, Y.; Wang, H.; Lim, A.; Ganteför, G.; Bowen, K. H.; Reveles, J. U.; Khanna, S. N. On the Existence of Designer Magnetic Superatoms. *J. Am. Chem. Soc.* **2013**, *135*, 4856–4861.
- (28) Ko, Y. J.; Shakya, A.; Wang, H.; Grubisic, A.; Zheng, W.; Götz, M.; Ganteför, G.; Bowen, K. H.; Jena, P.; Kiran, B. Electronic structure and properties of isoelectronic magic clusters: Al13X (X=H,Au,Li,Na,K,Rb,Cs). *J. Chem. Phys.* **2010**, *133*, 124308.
- (29) Zhang, X.; Ganteför, G.; Bowen, K. H.; Alexandrova, A. N. The PtAl-and PtAl₂-anions: Theoretical and photoelectron spectroscopic characterization. *J. Chem. Phys.* **2014**, *140*, 164316.
- (30) Wang, H.; Jae Ko, Y.; Zhang, X.; Ganteför, G.; Schnöckel, H.; Eichhorn, B. W.; Jena, P.; Kiran, B.; Kandalam, A. K.; Bowen, K. H. The Viability of Aluminum Zintl Anion Moieties within Magnesium-Aluminum Clusters. *J. Chem. Phys.* **2014**, *140*, 124309.
- (31) Wang, H.; Zhang, X.; Ko, Y. J.; Grubisic, A.; Li, X.; Ganteför, G.; Schnöckel, H.; Eichhorn, B. W.; Lee, M.-S.; Jena, P.; et al. Aluminum Zintl Anion Moieties Within Sodium Aluminum Clusters. *J. Chem. Phys.* **2014**, *140*, 054301.
- (32) Parr, R. G.; Yang, W. *Density-Functional Theory of Atoms and Molecules*; Oxford University Press: New York, 1989.
- (33) Becke, A. D. Density-functional thermochemistry. III. The role of exact exchange. *J. Chem. Phys.* **1993**, *98*, 5648–5652.
- (34) Lee, C.; Yang, W.; Parr, R. G. Development of the Colle-Salvetti Correlation-Energy Formula into a Functional of the Electron Density. *Phys. Rev. B: Condens. Matter Mater. Phys.* **1988**, *37*, 785–789.
- (35) Dunning, T. H., Jr Gaussian basis sets for use in correlated molecular calculations. I. The atoms boron through neon and hydrogen. *J. Chem. Phys.* **1989**, *90*, 1007–1023.
- (36) Kendall, R. A.; Dunning, T. H., Jr; Harrison, R. J. Electron affinities of the first-row atoms revisited. Systematic basis sets and wave functions. *J. Chem. Phys.* **1992**, *96*, 6796–6806.
- (37) Peterson, K. A. Correlation Consistent Basis Sets for Actinides. I. The Th and U Atoms. *J. Chem. Phys.* **2015**, *142*, 074105.
- (38) Weigand, A.; Cao, X.; Hankele, T.; Dolg, M. Relativistic Small-Core Pseudopotentials for Actinium, Thorium, and Protactinium. *J. Phys. Chem. A* **2014**, *118*, 2519–2530.
- (39) Peterson, K. A.; Puzzarini, C. Systematically Convergent Basis Sets for Transition Metals. II. Pseudopotential-based Correlation

- Consistent Basis Sets for the Group 11 (Cu, Ag, Au) and 12 (Zn, Cd, Hg) Elements. *Theor. Chem. Acc.* **2005**, *114*, 283–296.
- (40) Frisch, M. J.; Trucks, G. W.; Schlegel, H. B.; Scuseria, G. E.; Robb, M. A.; Cheeseman, J. R.; Scalmani, G.; Barone, V.; Petersson, G. A.; Nakatsuji, H.; et al. *Gaussian 16*, Revision A.03; Gaussian, Inc.: Wallingford CT, 2016.
- (41) Purvis, G. D., III; Bartlett, R. J. A full coupled-cluster singles and doubles model: The inclusion of disconnected triples. *J. Chem. Phys.* **1982**, *76*, 1910–1918.
- (42) Raghavachari, K.; Trucks, G. W.; Pople, J. A.; Head-Gordon, M. A Fifth-order Perturbation Comparison of Electron Correlation Theories. *Chem. Phys. Lett.* **1989**, *157*, 479–483.
- (43) Watts, J. D.; Gauss, J.; Bartlett, R. J. Coupled-cluster methods with noniterative triple excitations for restricted open-shell Hartree-Fock and other general single determinant reference functions. Energies and analytical gradients. *J. Chem. Phys.* **1993**, *98*, 8718–8733.
- (44) Bartlett, R. J.; Musiał, M. Coupled-Cluster Theory in Quantum Chemistry. *Rev. Mod. Phys.* **2007**, *79*, 291–352.
- (45) Feller, D.; Peterson, K. A.; Grant Hill, J. On the Effectiveness of CCSD(T) Complete Basis Set Extrapolations for Atomization Energies. *J. Chem. Phys.* **2011**, *135*, 044102.
- (46) Peterson, K. A.; Woon, D. E.; Dunning, T. H., Jr Benchmark calculations with correlated molecular wave functions. IV. The classical barrier height of the $\text{H}+\text{H}_2\rightarrow\text{H}_2+\text{H}$ reaction. *J. Chem. Phys.* **1994**, *100*, 7410–7415.
- (47) Dunham, J. L. The Energy Levels of a Rotating Vibrator. *Phys. Rev.* **1932**, *41*, 721–731.
- (48) Dunham, J. L. The Wentzel-Brillouin-Kramers Method of Solving the Wave Equation. *Phys. Rev.* **1932**, *41*, 713–720.
- (49) Moore, C. E. *Atomic Energy Levels as Derived from the Analysis of Optical Spectra, H to V*; U.S. National Bureau of Standards Circular 467; U.S. Department of Commerce, National Technical Information Service, COM-72-50282: Washington, D C, 1949; Vol. 1.
- (50) Sansonetti, J. E.; Martin, W. C. Handbook of Basic Atomic Spectroscopic Data. *J. Phys. Chem. Ref. Data* **2005**, *34*, 1559–2259.
- (51) <https://atct.anl.gov/Thermochemical%20Data/version%201.122g/index.php> (accessed January 18, 2019).
- (52) Ruscic, B.; Pinzon, R. E.; Morton, M. L.; von Laszewski, G.; Bittner, S. J.; Nijssure, S. G.; Amin, K. A.; Minkoff, M.; Wagner, A. F. Introduction to Active Thermochemical Tables: Several “Key” Enthalpies of Formation Revisited†. *J. Phys. Chem. A* **2004**, *108*, 9979–9997.
- (53) Changala, P. B.; Nguyen, T. L.; Baraban, J. H.; Ellison, G. B.; Stanton, J. F.; Bross, D. H.; Ruscic, B. Active Thermochemical Tables: The Adiabatic Ionization Energy of Hydrogen Peroxide. *J. Phys. Chem. A* **2017**, *121*, 8799–8806.
- (54) Luo, Y.-R. *Comprehensive Handbook of Chemical Bond Energies*; CRC Press, Taylor and Francis Group: Boca Raton, FL, 2007.
- (55) Cox, J. D.; Wagman, D. D.; Medvedev, V. A. *CODATA Key Values for Thermodynamics*; Hemisphere Publishing Corp.: New York, 1989.
- (56) *Thermal Constants of Substances*; Yungman, V. S., Glushko, V. P., Medvedev, V. A., Gurvich, L. V., Eds.; Wiley: New York, 1999; Vol. 8.
- (57) Curtiss, L. A.; Raghavachari, K.; Redfern, P. C.; Pople, J. A. Assessment of Gaussian-2 and Density Functional Theories for the Computation of Enthalpies of Formation. *J. Chem. Phys.* **1997**, *106*, 1063–1079.
- (58) Deegan, M. J. O.; Knowles, P. J. Perturbative Corrections to Account for Triple Excitations in Closed and Open Shell Coupled Cluster Theories. *Chem. Phys. Lett.* **1994**, *227*, 321–326.
- (59) Rittby, M.; Bartlett, R. J. An open-shell spin-restricted coupled cluster method: application to ionization potentials in nitrogen. *J. Phys. Chem.* **1988**, *92*, 3033–3036.
- (60) Knowles, P. J.; Hampel, C.; Werner, H. J. Coupled Cluster Theory for High Spin, Open Shell Reference Wave Functions. *J. Chem. Phys.* **1993**, *99*, 5219–5227.
- (61) Werner, H.-J.; Knowles, P. J.; Knizia, G.; Manby, F. R.; Schütz, M.; Celani, P.; Györffy, W.; Kats, T.; Korona, T.; Lindh, R.; et al. MOLPRO, Version 2018.1 a Package of ab Initio Programs. <http://www.molpro.net> (accessed April 15, 2020).
- (62) Werner, H.-J.; Knowles, P. J.; Knizia, G.; Manby, F. R.; Schütz, M. Molpro: a general-purpose quantum chemistry program package. *Wiley Interdiscip. Rev.: Comput. Mol. Sci.* **2012**, *2*, 242–253.
- (63) Reed, A. E.; Curtiss, L. A.; Weinhold, F. Intermolecular Interactions from a Natural Bond Orbital, Donor-Acceptor Viewpoint. *Chem. Rev.* **1988**, *88*, 899–926.
- (64) Weinhold, F.; Landis, C. R. *Valency and Bonding: A Natural Bond Orbital Donor–Acceptor Perspective*; University Press: Cambridge, U.K., 2005.
- (65) Glendening, E. D.; Badenhoop, J. K.; Reed, A. E.; Carpenter, J. E.; Bohmann, J. A.; Morales, C. M.; Karafiloglu, P.; Landis, C. R.; Weinhold, F. *Natural Bond Order 7.0*; Theoretical Chemistry Institute, University of Wisconsin: Madison, WI, 2018.
- (66) Glendening, E. D.; Landis, C. R.; Weinhold, F. NBO 7.0: New Vistas in Localized and Delocalized Chemical Bonding Theory. *J. Comput. Chem.* **2019**, *40*, 2234–2241.
- (67) Ichino, T.; Gianola, A. J.; Andrews, D. H.; Lineberger, W. C. Photoelectron Spectroscopy of AuO-and AuS-. *J. Phys. Chem. A* **2004**, *108*, 11307–11313.
- (68) Hotop, H.; Lineberger, W. C. Dye-laser photodetachment studies of Au-, Pt-, PtN-, and Ag-. *J. Chem. Phys.* **1973**, *58*, 2379–2387.
- (69) Tang, R.; Si, R.; Fei, Z.; Fu, X.; Lu, Y.; Brage, T.; Liu, H.; Chen, C.; Ning, C. Candidate for Laser Cooling of a Negative Ion: High-Resolution Photoelectron Imaging of Th^- . *Phys. Rev. Lett.* **2019**, *123*, 203002.
- (70) Konigs, R. J. M.; Morss, L. R.; Fuger, J. *Thermodynamic Properties of Actinides and Actinide Compounds in The Chemistry of the Actinide and Transactinide Elements*, 3rd ed.; Morss, L. R., Edelstein, N. M., Fuger, J., Eds.; Springer: Dordrecht, 2006; Chapter 19, Vol. 4, pp 2113–2224.
- (71) Thanthiriwatte, K. S.; Vasiliu, M.; Battey, S. R.; Lu, Q.; Peterson, K. A.; Andrews, L.; Dixon, D. A. Gas Phase Properties of MX₂and MX₄(X = F, Cl) for M = Group 4, Group 14, Cerium, and Thorium. *J. Phys. Chem. A* **2015**, *119*, 5790–5803.
- (72) Pyykkö, P. Additive Covalent Radii for Single-, Double-, and Triple-Bonded Molecules and Tetrahedrally Bonded Crystals: A Summary. *J. Phys. Chem. A* **2015**, *119*, 2326–2337.
- (73) Kramida, A.; Ralchenko, Y.; Reader, J.; The NIST ASD Team. *NIST Atomic Spectra Database* (ver. 5.7.1), [Online]; National Institute of Standards and Technology: Gaithersburg, MD, 2019. Available: <https://physics.nist.gov/asd>. DOI: 10.18434/T4W30F. (accessed August 6, 2020).
- (74) Gagliardi, L. When Does Gold Behave as a Halogen? Predicted Uranium Tetrauride and Other MAu₄Tetrahedral Species, (M = Ti, Zr, Hf, Th). *J. Am. Chem. Soc.* **2003**, *125*, 7504–7505.
- (75) Pyykkö, P. Relativity, Gold, Closed-Shell Interactions, and CsAu-NH₃. *Angew. Chem., Int. Ed.* **2002**, *41*, 3573–3578.
- (76) Pyykkö, P. Theoretical Chemistry of Gold. II. *Inorg. Chim. Acta* **2005**, *358*, 4113–4130.
- (77) Pyykkö, P. Theoretical Chemistry of Gold. III. *Chem. Soc. Rev.* **2008**, *37*, 1967–1997.
- (78) Persaud, R. R.; Chen, M.; Peterson, K. A.; Dixon, D. A. Potential Energy Surface of Group 11 Trimers (Cu, Ag, Au): Bond Angle Isomerism in Au₃. *J. Phys. Chem. A* **2019**, *123*, 1198–1207.
- (79) Emsley, J. *The Elements*, 2nd ed.; Clarendon Press: Oxford, U.K., 1994.